BOLIDE IMPACTS AND THE OXIDATION STATE OF CARBON IN THE EARTH'S EARLY ATMOSPHERE

JAMES F. KASTING

Department of Geosciences, The Pennsylvania State University, University Park, PA 16802, U.S.A.

(Received November 2, 1989)

Abstract. A one-dimensional photochemical model was used to examine the effect of bolide impacts on the oxidation state of Earth's primitive atmosphere. The impact rate should have been high prior to 3.8 Ga before present, based on evidence derived from the Moon. Impacts of comets or carbonaceous asteroids should have enhanced the atmospheric CO/CO_2 ratio by bringing in CO ice and/or organic carbon that can be oxidized to CO in the impact plume. Ordinary chondritic impactors would contain elemental iron that could have reacted with ambient CO_2 to give CO. Nitric oxide (NO) should also have been produced by reaction between ambient CO_2 and N_2 in the hot impact plumes. High NO concentrations increase the atmospheric CO/CO_2 ratio by increasing the rainout rate of oxidized gases. According to the model, atmospheric CO/CO_2 ratios of unity or greater are possible during the first several hundred million years of Earth's history, provided that dissolved CO was not rapidly oxidized to bicarbonate in the ocean. Specifically, high atmospheric CO/CO_2 ratios are possible if either: (1) the climate was cool (like today's climate), so that hydration of dissolved CO to formate was slow, or (2) the formate formed from CO was efficiently converted into volatile, reduced carbon compounds, such as methane. A high atmospheric CO/CO_2 ratio may have helped to facilitate prebiotic synthesis by enhancing the production rates of hydrogen cyanide and formaldehyde. Formaldehyde may have been produced even more efficiently by photochemical reduction of bicarbonate and formate in Fe^{++}-rich surface waters.

1. Introduction

The composition of Earth's primitive atmosphere has been a topic of investigation for many years because of its possible influence on the origin of life. The debate over this issue has swung back and forth (Chang *et al.*, 1983). As early as 1919, Osborne (cited in Oparin, 1938) assumed that the early earth was 'thickly blanketed with ... water vapor and carbon dioxide'. This idea fell out of favor as Oparin (1938) and then Urey (1952) proposed that the primitive atmosphere consisted of molecular hydrogen, ammonia, methane, and other hydrocarbons. Their theory was supported by the laboratory work of Miller (1953, 1955), which demonstrated that amino acids and other organic compounds could be readily produced by spark discharges under these highly reducing conditions.

The Oparin-Urey model was challenged by Rubey (1951, 1955), who pointed out that modern volcanic gases are dominated by CO_2, rather than CH_4. Rubey suggested that the early atmosphere was rather like the present atmosphere, except that it lacked free O_2. Holland (1962) showed thermodynamically that CO_2 should dominate volcanic emissions once the crust was free of metallic iron. The concept of a CO_2-rich primitive atmosphere received additional support from photochemists, who demonstrated that methane and carbon monoxide would have been

Origins of Life and Evolution of the Biosphere **20**: 199–231, 1990.

rapidly oxidized to CO_2 by OH radicals produced from water vapor photolysis (Walker, 1977; Yung and McElroy, 1979; Levine, 1982; Kasting *et al.*, 1983), and from climatologists, who argued that enhanced CO_2 concentrations were the best way of compensating for the faint young sun (Owen *et al.*, 1979; Walker *et al.*, 1981; Kasting *et al.*, 1988). A CO_2-rich atmosphere is also what one would expect from looking at the atmospheres of Mars and Venus, both of which are more than 95% CO_2 (von Zahn *et al.*, 1983; McElroy *et al.*, 1977).

The photochemical argument in favor of a CO_2-dominated early atmosphere goes as follows: CO_2 photodissociates readily at wavelengths shorter than ~200 nm

$$CO_2 + h\nu \rightarrow CO + O\,. \tag{R73}$$

The direct recombination of CO with O is spin-forbidden, and therefore slow; however, the reaction of CO with OH radicals produced from water vapor photolysis is fast

$$H_2O + h\nu \rightarrow H + OH \tag{R72}$$

$$CO + OH \rightarrow CO_2 + H \tag{R110}$$

The presence of water vapor in the primitive terrestrial atmosphere should have kept the CO abundance low, just as it does in the present Martian atmosphere (McElroy and Donahue, 1972). [Sulfur and chlorine compounds are thought to catalyze CO recombination on Venus (Yung and DeMore, 1982)]. CO/CO_2 ratios predicted for early Earth are of the order of 10^{-4} or below (Yung and McElroy, 1979; Pinto *et al.*, 1980; Kasting *et al.*, 1984; Levine and Augustsson, 1985).

Previous photochemical models, however, have explored only a limited range of CO_2 partial pressures (generally less than 0.2 bar) and have ignored the effects of impacts. The actual CO_2 partial pressure on an ocean-covered early Earth could have been as high as 10 bars (Walker, 1985). Large CO_2 amounts can slow the rate of CO recombination by shielding water vapor from photolysis. At the same time, impacts could have had an appreciable influence on atmospheric composition (Fegley *et al.*, 1986; Prinn and Fegley, 1987), but this has not been factored into photochemical model calculations.

Here, I suggest that the two major effects of impacts would have been to produce excess CO and NO. I then incorporate impact production of these species into a one-dimensional photochemical model and discuss the possible consequences for atmospheric photochemistry and for the origin of life.

2. Production of CO and NO by impacts

a. Impact rate

Observations of craters on the Moon's surface and dating of lunar rocks returned by the Apollo missions indicate that the Moon, and by implication the Earth as well, was heavily bombarded prior to ~3.8 Ga. Recent estimates of the impact

rate have been derived from the cratering record (Maher and Stevenson, 1988; Chyba, 1989) and from geochemical anomalies, principally Ir, in the lunar crust (Sleep *et al.*, 1989). The latter method yields the integrated amount of impact material accreted between 4.44 Ga (the age of solidification of the upper parts of the lunar crust) and 3.8 Ga (the age of the youngest large craters). This can be converted into an impact rate in g yr^{-1} if one uses the cratering record to estimate the time dependence of the impact flux.

According to Sleep *et al.* (1989), the total amount of material accreted by the Moon between 3.8 and 4.44 Ga is equivalent to a layer ~0.7 km in thickness. This estimate may be too low by a factor of two because at least half of the mass of a typical bolide escapes from the Moon's small gravitational field (Chyba, 1989). Because of its higher gravity and larger surface area, the Earth should accrete at least 23 times as much material as the Moon, or possibly more if the impactor size distribution is skewed toward large bodies (Sleep *et al.*, 1989). Thus, the equivalent thickness of the material accreted by the Earth between 3.8 and 4.44 Ga is at least 2.4 km (twice the Sleep *et al.*, estimate). For an assumed density of 3 g cm^{-3}, this yields a total accreted mass (M_{tot}) of $\sim 4 \times 10^{24}$ g.

The time dependence of the impact flux is uncertain. The cratering estimates of Wilhelms (1984) imply an exponential fall off with a decay constant of 70 Ma (Maher and Stevenson, 1988). Cratering data derived by the Basaltic Volcanism Study Project (BVSP, 1981) imply a time constant of 144 Ma (Chyba, 1989) to 220 Ma (Melosh and Vickery, 1989). None of these time constants can be considered reliable, since the impact flux probably did not follow a simple exponential decay law (Chyba, 1989; Grinspoon and Sagan, 1989). Unfortunately, one does not know what the actual decay law was. For the sake of concreteness, I have chosen to approximate the impact flux as

$$F(t) = F_0 \exp[(t - t_0)/0.2] , \tag{1}$$

where t = time before present in billions of years and t_0 is taken at 3.8 Ga. F_0 is the mass flux at 3.8 Ga, which is equal to 8×10^{14} g yr^{-1} for the assumed value of M_{tot}. This value of F_0 is consistent with the impact flux of 0.2–0.4 km^3 yr^{-1}, or (6–12) $\times 10^{14}$ g yr^{-1}, that would cause complete subduction of terrigenous sediments and might therefore explain the absence of crustal rocks older than about 3.8 Ga (Koster van Groos, 1988).

b. CO PRODUCTION RATE

One likely effect of impacts would have been to act as a source for carbon monoxide, CO. CO could have been supplied in at least three different ways. The first two of these are relatively straightforward. If the impactors were comets, CO would have been brought in directly as one of the major icy constituents (Jessberger *et al.*, 1989). Alternatively, if the impactors were of chondritic composition, they would have contained organic carbon, much of which should have been oxidized to CO in the impact plume. The actual organic compounds themselves are preserved only

over a limited range of impactor masses ($< 10^5$ kg), for which atmospheric aerobraking is effective (Anders, 1989). As discussed below, most of the incoming mass was probably in larger bodies, which would have passed unimpeded through the atmosphere and been vaporized on hitting the surface (Melosh and Vickery, 1989; Sleep *et al.*, 1989).Organic matter in the hot rock vapor plume should have combined with oxygen derived from silicates, water, or ambient atmospheric CO_2 to give CO. Very little of it would have been directly oxidized to CO_2 because of the low oxygen fugacity of both the impactor and the Earth's crust. For large incoming bodies, nearly quantitative conversion of organic carbon to CO seems likely.

A third mechanism for CO production could be important for more reduced impactors, such as ordinary chondrites. In this case, hot metallic iron in the plume should react with ambient atmospheric CO_2

$$Fe + CO_2 \rightarrow FeO + CO\ .$$

The reaction is endothermic at high temperatures, but becomes thermodynamically favorable once the iron vapor has condensed. A typical impact plume would have consisted largely of silicate vapor, which condenses at ~2000 K for typical atmospheric pressures (Sleep *et al.*, 1989). Iron droplets within the silicate plume would presumably have been maintained at about this same temperature, roughly 200 K above their cristallization point (Stull and Prophet, 1971). The outer layers of these droplets would have reacted with atmospheric CO_2 to form liquid FeO. (The crystallization temperature for FeO is 1650 K.) As long as the droplets remained liquid, fresh iron would presumably have been brought to their surfaces to continue the reaction. Since $pCO/pCO_2 \approx 10$ for the above reaction at 2000 K (Stull and Phophet, 1971), most of the CO_2 molecules encountered by the droplet during its residence time in the plume should have been converted to CO. The larger impact plumes may have persisted from days to months (Sleep *et al.*, 1989); hence, most of the iron should have had sufficient time to react. I therefore assume that the reaction between iron and CO_2 would have proceeded quantitatively. The reader can scale down these numbers if he thinks this conversion efficiency is too high, as the results are presented in parametric form.

The amount of CO produced clearly depends on the nature of the planetesimals that were hitting the early Earth. Rather than trying to guess what they were, I estimate the CO source for three different types of impactors: ordinary chondrites, Cl carbonaceous chondrites, and comets. Ordinary and Cl chondrites contain about 0.1% and 3% carbon by weight, respectively (Lewis and Prinn, 1984). Using the mass flux F_0 given above, the carbon in these bodies would generate CO fluxes of 2.5×10^8 cm^{-2} s^{-1} and 7.5×10^9 cm^{-2} s^{-1}, respectively, at 3.8 Ga. Comets are somewhat richer in carbon: the C/H_2O ratio in the coma of Comet Halley is ~0.2 by volume, or 0.13 by mass (Krankowsky and Eberhardt, 1988). For an assumed gas/dust mass ratio of 1 (Jessberger *et al.*, 1989), this yields an overall carbon content of ~ 6% by weight. Thus, the predicted CO flux at 3.8 Ga for cometary

impactors is 1.5×10^{10} cm^{-2} s^{-1}.

Most of the CO production by ordinary chondritic impactors would come from the reaction of iron with CO_2. Ordinary chondrites typically contain 5–15% Fe by weight (Lewis and Prinn, 1984). Using the 5% value and assuming quantitative reaction of Fe with CO_2 yields a CO flux at 3.8 Ga of 2.7×10^9 cm^{-2} s^{-1}.

c. NO PRODUCTION RATE

NO would also have been produced in impacts by shock heating of ambient N_2 and CO_2 (Chameides and Walker, 1981; Fegley *et al.*, 1986). This process can be simulated with various degrees of complexity. I consider the simplest one first. The NO yield for N_2–O_2 atmospheres is thought to be $\sim 3 \times 10^8$ molecules erg^{-1} (Prinn and Fegley, 1987). The predicted yield for N_2–CO_2 atmospheres is about half this value, given a freeze-out temperature of 3500 K (Kasting, 1979). For a typical asteroidal body during the late accretionary period, the impact velocity would have been ~17 km s^{-1} (Sleep *et al.*, 1989), so the energy released is 1.5×10^{12} erg g^{-1}. Combining these figures with the estimated accretionary mass flux gives an NO flux of 1.1×10^9 cm^{-2} s^{-1} at 3.8 Ga.

A more elaborate treatment of impacts indicates that the NO yield per erg decreases as the energy of the impact increases (Zahnle, 1990). Thus, the NO production rate should depend on the size of the incoming planetesimals. A reasonable size distribution for an assemblage of bodies affected by accretion and fragmentation is (Safronov and Ruzmaikina, 1986; Sleep *et al.*, 1989)

$$n(M)\mathrm{d}M = C\,M^{-q}\mathrm{d}M\,, \tag{2}$$

where $n(M)$ is the number of bodies with masses between M and $M + \mathrm{d}M$ and C is a constant. The expected value of q ranges from 1.67 to 2. Lower values of q imply that the mass is concentrated mostly in the larger bodies. I choose a value of 1.7 here; this should produce a minimum estimate for NO production.

Since the energy E of an impactor is proportional to its mass, one may also write

$$n(E)\mathrm{d}E = C'\,\mathrm{E}^{-q}\mathrm{d}E\,. \tag{3}$$

The average NO yield per unit impact energy for the swarm is given by

$$P_{\mathrm{av}}(\mathrm{NO}) = \frac{\int_0^{E_{\max}} P_{NO}(E)\,n(E)\,E\mathrm{d}E}{\int_0^{E_{\max}} n(E)\,E\mathrm{d}E} \tag{4}$$

where $E_{\max}$ is the energy of the largest impact event. I assume that the impacts occur at 17 km s^{-1} and that the mass of the largest impactor is 2×10^{22} g, or ten times the estimated mass of the object that formed the Imbrium crater on the Moon (Sleep *et al.*, 1989).

Zahnle's results for $P_{NO}(E)$ for an oceanic impact (his Figure 3) can be expressed in analytic form by dividing the energy scale into 4 different regions and writing

$$P_{NO}(E) = A_i \, E^{Bi} \tag{5}$$

in each one. $P_{av}(NO)$ can then be calculated by performing the integrations in Equation (4) over each separate interval and then summing the results. This yields $P_{av}(NO) = 3.3 \times 10^7$ molecules erg^{-1}, or roughly one-tenth Prinn and Fegley's suggested value. The corresponding NO flux at 3.8 Ga is 1.2×10^8 cm^{-2} s^{-1}. If E_{max} is assumed to be ten times smaller, the calculated NO flux is about 70% higher. The actual NO production efficiency was probably somewhere between the value calculated by this method and the higher value based on Prinn and Fegley's analysis.

3. Photochemical Model

To determine the significance of impact production of CO and NO, it is necessary to incorporate their production rates into a model of atmospheric photochemistry. The model used in this study is a one-dimensional (horizontally-averaged) model similar to those used in previous studies (e.g. Kasting *et al.*, 1984; Kasting *et al.*, 1989). A brief description of the model follows.

a. Chemistry and numerical procedures

The background atmosphere considered in the model consists of 0.8 bar of N_2

TABLE I

Chemical species included in the model

Long-lived species[a]				
O	HO_2	H_2CO	SO_2	S_2
O_2	H_2O_2	NO	HSO	H_2SO_4
H_2O	H_2	NO_2	H_2S	Particulate sulfate
H	CO	HNO	HS	Particulate sulfur
OH	HCO	SO	S	
Short-lived species[b]				
O_3	HNO_2	S_4	$SO_2(^1B)$	
$O(^1D)$	HNO_3	SO_3	HSO_3	
N	S_3	$SO_2(^3B)$		
Relatively inert				
CO_2	N_2			

[a] Chemistry and transport considered.

[b] Chemistry only.

(Classification into long- and short-lived species depends both upon chemical lifetime and the degree of nonlinearity of the chemistry. Some of the 'long-lived' species actually have very short photochemical lifetimes).

TABLE II

Reactions and rate constants

	Reaction	Rate constant ($cm^3\ s^{-1}$)	Reference	Notes
Sulfur chemistry				
R1)	$SO_2 + h\nu \rightarrow SO + 0$	$1.31 \times 10^{-4}\ s^{-1}$	Warneck *et al.*, 1964;	a
R2)	$SO_2 + h\nu \rightarrow SO_2(^1B)$	$1.62 \times 10^{-3}\ s^{-1}$	Okabe, 1971	a
R3)	$SO_2 + h\nu \rightarrow SO_2(^3B)$	$9.49 \times 10^{-7}\ s^{-1}$		a
R4)	$SO + h\nu \rightarrow S + O$	$3.98 \times 10^{-4}\ s^{-1}$	Phillips *et al.*, 1981	a,m
R5)	$H_2S + h\nu \rightarrow HS + H$	$2.27 \times 10^{-4}\ s^{-1}$	Sullivan and Holland, 1966	a
R6)	$SO_3 + h\nu \rightarrow SO_2 + O$	0		b
R7)	$H_2SO_4 + h\nu \rightarrow SO_2 + 2\ OH$	$5.00 \times 10^{-7}\ s^{-1}$	Turco *et al.*, 1979	c
R8)	$HSO + h\nu \rightarrow HS + O$	$(= J_{HO_2})$	See R79	d
R9)	$S_2 + h\nu \rightarrow S + S$	$1.00 \times 10^{-3}\ s^{-1}$	deAlmeida and Singh, 1986	e
R10)	$S_2 + h\nu \rightarrow S_2^*$	0		f
R11)	$S_3 + h\nu \rightarrow S_2 + S$	$(= J_{S_2})$	See R9	d
R12)	$S_4 + h\nu \rightarrow S_2 + S_2$	$(= J_{S_2})$	See R9	d
R13)	$SO_2(^1B) + M \rightarrow SO_2(^3B) + M$	1×10^{-12}	Turco *et al.*, 1982	
R14)	$SO_2(^1B) + M \rightarrow SO_2 + M$	1×10^{-11}	Turco *et al.*, 1982	
R15)	$SO_2(^1B) \rightarrow SO_2(^3B) + h\nu$	$1.5 \times 10^{3}\ s^{-1}$	Turco *et al.*, 1982	
R16)	$SO_2(^1B) \rightarrow SO_2 + h\nu$	$2.2 \times 10^{4}\ s^{-1}$	Turco *et al.*, 1982	
R17)	$SO_2(^1B) + O_2 \rightarrow SO_3 + O$	1×10^{-16}	Turco *et al.*, 1982	
R18)	$SO_2(^1B) + SO_2 \rightarrow SO_3 + SO$	4×10^{-12}	Turco *et al.*, 1982	
R19)	$SO_2(^3B) + M \rightarrow SO_2 + M$	1.5×10^{-13}	Turco *et al.*, 1982	
R20)	$SO_2(^3B) \rightarrow SO_2 + h\nu$	$1.13 \times 10^{3}\ s^{-1}$	Turco *et al.*, 1982	
R21)	$SO_2(^3B) + SO_2 \rightarrow SO_3 + SO$	7×10^{-14}	Turco *et al.*, 1982	
R22)	$SO_2 + OH + M \rightarrow HSO_3 + M$	$k_0 = 3 \times 10^{-31}$; $n = 3.3$ $k_1 = 1.5 \times 10^{-12}$; $m = 0$	DeMore *et al.*, 1985	g
R23)	$SO_2 + O + M \rightarrow SO_3 + M$	3.4×10^{-32} exp(−1130/T)[M]	Turco *et al.*, 1982	
R24)	$SO + O_2 \rightarrow SO_2 + O$	2.4×10^{-13} exp(−2370/T)	DeMore *et al.*, 1985	
R25)	$SO + HO_2 \rightarrow SO_2 + OH$	2.3×10^{-11}	Yung and DeMore, 1982	h
R26)	$SO + O + M \rightarrow SO_2 + M$	6×10^{-31} [M]		d
R27)	$SO + OH \rightarrow SO_2 + H$	8.6×10^{-11}	DeMore *et al.*, 1985	
R28)	$SO + NO_2 \rightarrow SO_2 + NO$	1.4×10^{-11}	DeMore *et al.*, 1985	
R29)	$SO + O_3 \rightarrow SO_2 + O_2$	3.6×10^{-12} exp(−1100/T)	DeMore *et al.*, 1985	
R30)	$SO + SO \rightarrow SO_2 - S$	8.3×10^{-15}	Herron and Huie, 1980	
R31)	$SO + SO_3 \rightarrow 2\ SO_2$	2×10^{-15}	Yung and DeMore, 1982	d
R32)	$SO + HCO \rightarrow HSO + CO$	$(= k_{118})$		d
R33)	$H + SO + M \rightarrow HSO + M$	$(= k_{89})$		d
R34)	$HSO_3 + O_2 \rightarrow SO_3 + HO_2$	1×10^{-11} exp(−1000/T)	Toon *et al.*, 1987	d
R35)	$HSO_3 + OH \rightarrow SO_3 + H_2O$	1×10^{-11}		d
R36)	$HSO_3 + H \rightarrow SO_3 + H_2$	1×10^{-11}		d
R37)	$HSO_3 + O \rightarrow SO_3 + OH$	1×10^{-11}		d
R38)	$SO_3 + H_2O \rightarrow H_2SO_4$	9×10^{-13}		d
R39)	$H_2S + OH \rightarrow HS + H_2O$	5.9×10^{-12} exp(−65/T)	DeMore *et al.*, 1985	
R40)	$H_2S + H \rightarrow HS + H_2$	1.3×10^{-11} exp(−860/T)	Baulch *et al.*, 1976	
R41)	$H_2S + O \rightarrow HS + OH$	1×10^{-11} exp(−1810/T)	DeMore *et al.*, 1985	
R42)	$HS + O \rightarrow SO + H$	5×10^{-11}		d
R43)	$HS + O_2 \rightarrow SO + OH$	5×10^{-19}	Toon *et al.*, 1987	d

Table II. (Continued).

	Reaction	Rate constant ($cm^3\ s^{-1}$)	Reference	Notes
R44)	$HS + HO_2 \rightarrow H_2S + O_2$	3×10^{-11}	McElroy *et al.*, 1980	d
R45)	$HS + HS \rightarrow H_2S + S$	1.2×10^{-11}	Baulch *et al.*, 1976	
R46)	$HS + HCO \rightarrow H_2S + CO$	5×10^{-11}		d
R47)	$HS + H \rightarrow H_2 + S$	1.0×10^{-11}	Langford and Oldershaw, 1972	
R48)	$HS + S \rightarrow S_2 + H$	$(= k_{95})$		d
R49)	$HS + O_3 \rightarrow HSO + O_2$	3.2×10^{-12}	DeMore *et al.*, 1985	
R50)	$HS + NO_2 \rightarrow HSO + NO$	3.2×10^{-11}	DeMore *et al.*, 1985	
R51)	$HS + H_2CO \rightarrow H_2S + HCO$	$1.7 \times 10^{-11} \exp(-800/T)$	DeMore *et al.*, 1985	i
R52)	$S + O_2 \rightarrow SO + O$	2.3×10^{-12}	DeMore *et al.*, 1985	
R53)	$S + OH \rightarrow SO + H$	6.6×10^{-11}	DeMore *et al.*, 1985	
R54)	$S + HCO \rightarrow HS + CO$	5×10^{-11}		d
R55)	$S + HO_2 \rightarrow HS + O_2$	1.5×10^{-11}		d
R56)	$S + HO_2 \rightarrow SO + OH$	1.5×10^{-11}		d
R57)	$S + O_3 \rightarrow SO + O_2$	1.2×10^{-11}	DeMore *et al.*, 1985	
R58)	$S + CO_2 \rightarrow SO + CO$	1×10^{-20}	Yung and DeMore, 1982	d
R59)	$S + S + M \rightarrow S_2 + M$	$(= k_{108})$		d
R60)	$S + S_2 + M \rightarrow S_3 + M$	$2.8 \times 10^{-32}\ [M]$		d
R61)	$S + S_3 + M \rightarrow S_4 + M$	$(= k_{63})$		d
R62)	$S_2 + O \rightarrow S + SO$	1.1×10^{-11}	Hills *et al.*, 1987	
R63)	$S_2 + S_2 + M \rightarrow S_4 + M$	$2.8 \times 10^{-31}\ [M]$	Baulch *et al.*, 1976	j
R64)	$S_4 + S_4 + M \rightarrow S_8 + M$	$(= k_{63})$		d
R65)	$HSO + NO \rightarrow HNO + SO$	$(= k_{132})$		d
R66)	$HSO + OH \rightarrow H_2O + SO$	$(= k_{96})$		d
R67)	$HSO + H \rightarrow HS + OH$	$(= k_{92})$		d
R68)	$HSO + H \rightarrow H_2 + SO$	$(= k_{90})$		d
R69)	$HSO + HS \rightarrow H_2S + SO$	1×10^{-12}		d
R70)	$HSO + O \rightarrow OH + SO$	$(= k_{100})$		d
R71)	$HSO + S \rightarrow HS + SO$	1×10^{-11}		d
O_x-HO_x-H_xCO chemistry				
R72)	$H_2O + h\nu \rightarrow H + OH$	$2.50 \times 10^{-6}\ s^{-1}$	Thompson *et al.*, 1963	a
R73)	$CO_2 + h\nu \rightarrow CO + O$	$1.23 \times 10^{-9}\ s^{-1}$	Shemansky, 1972	a
R74)	$CO_2 + h\nu \rightarrow CO + O(^1D)$	$5.89 \times 10^{-9}\ s^{-1}$	Thompson *et al.*, 1963	a
R75)	$O_2 + h\nu \rightarrow O + O$	$4.10 \times 10^{-8}\ s^{-1}$	Allen and Frederick, 1982	a
R76)	$O_2 + h\nu \rightarrow O + O(^1D)$	$1.16 \times 10^{-7}\ s^{-1}$	Thompson *et al.*, 1963	a
R77)	$O_3 + h\nu \rightarrow O_2 + O$	$1.38 \times 10^{-3}\ s^{-1}$	WMO, 1985	a
R78)	$O_3 + h\nu \rightarrow O_2 + O(^1D)$	$5.21 \times 10^{-3}\ s^{-1}$	WMO, 1985	a
R79)	$HO_2 + h\nu \rightarrow OH + O$	$5.48 \times 10^{-4}\ s^{-1}$	DeMore *et al.*, 1985	a
R80)	$H_2O_2 + h\nu \rightarrow OH + OH$	$8.17 \times 10^{-5}\ s^{-1}$	DeMore *et al.*, 1985	a
R81)	$H_2CO + h\nu \rightarrow HCO + H$	$6.19 \times 10^{-5}\ s^{-1}$	DeMore *et al.*, 1985	a
R82)	$H_2CO + h\nu \rightarrow H_2 + CO$	$5.19 \times 10^{-5}\ s^{-1}$	DeMore *et al.*, 1985	a
R83)	$HCO + h\nu \rightarrow H + CO$	$1 \times 10^{-2}\ s^{-1}$	Pinto *et al.*, 1980	d
R84)	$H_2O + O(^1D) \rightarrow OH + OH$	2.2×10^{-10}	DeMore *et al.*, 1985	
R85)	$H_2 + O(^1D) \rightarrow OH + H$	1×10^{-10}	DeMore *et al.*, 1985	
R86)	$H_2 + O \rightarrow OH + H$	$3 \times 10^{-14}\ T \exp(-4480/T)$	Hampson and Garvin, 1977	
R87)	$H_2 + OH \rightarrow H_2O + H$	$6.1 \times 10^{-12} \exp(-2030/T)$	DeMore *et al.*, 1985	
R88)	$H + O_3 \rightarrow OH + O_2$	$1.4 \times 10^{-10} \exp(-470/T)$	DeMore *et al.*, 1985	

Table II. (Continued).

	Reaction	Rate constant ($cm^3\ s^{-1}$)	Reference	Notes
R89)	$H + O_2 + M \rightarrow HO_2 + M$	$k_0 = 5.5 \times 10^{-32}$; $n = 1.6$ $k_\iota = 7.5 \times 10^{-11}$; $m = 0$	DeMore *et al.*, 1985	g
R90)	$H + HO_2 \rightarrow H_2 + O_2$	7.4×10^{-11} ($\times 0.09$)	DeMore *et al.*, 1985	
R91)	$H + HO_2 \rightarrow H_2O + O$	7.4×10^{-11} ($\times 0.04$)	DeMore *et al.*, 1985	
R92)	$H + HO_2 \rightarrow OH + OH$	7.4×10^{-11} ($\times 0.87$)	DeMore *et al.*, 1985	
R93)	$H + H + M \rightarrow H_2 + M$	9.1×10^{-33} $(T/300)^{-1.33}[M]$	Hochanadel *et al.*, 1980	
R94)	$H + OH + M \rightarrow H_2O + M$	$6.1 \times 10^{-26}\ T^{-2}\ [M]$	McEwan and Phillips, 1975	
R95)	$OH + O \rightarrow H + O_2$	$2.2 \times 10^{-11} \exp(117/T)$	DeMore *et al.*, 1985	
R96)	$OH + HO_2 \rightarrow H_2O + O_2$	$1.7 \times 10^{-11} \exp(416/T)$ $+ 3 \times 10^{-31}$ $\exp(500/T)[M]$	DeMore *et al.*, 1985	
R97)	$OH + O_3 \rightarrow HO_2 + O_2$	$1.6 \times 10^{-12} \exp(-940/T)$	DeMore *et al.*, 1985	
R98)	$OH + OH + M \rightarrow H_2O_2 + M$	$k_0 = 6.9 \times 10^{-31}$; $n = 0.8$ $k_\iota = 1 \times 10^{-11}$; $m = 1$	DeMore *et al.*, 1985	g
R99)	$OH + OH \rightarrow H_2O + O$	$4.2 \times 10^{-12} \exp(-242/T)$	DeMore *et al.*, 1985	
R100)	$HO_2 + O \rightarrow OH + O_2$	$3 \times 10^{-11} \exp(200/T)$	DeMore *et al.*, 1985	
R101	$HO_2 + O_3 \rightarrow OH + O_2$	$1.4 \times 10^{-14} \exp(-580/T)$	DeMore *et al.*, 1985	
R102)	$HO_2 + HO_2 \rightarrow H_2O_2 + O_2$	$2.3 \times 10^{-13} \exp(590/T)$ $+ 1.7 \times 10^{-33}$ $\exp(1000/T)[M]$	DeMore *et al.*, 1985	
R103)	$H_2O_2 + OH \rightarrow HO_2 + H_2O$	$3.1 \times 10^{-12} \exp(-187/T)$	DeMore *et al.*, 1985	
R105)	$O(^1D) + N_2 \rightarrow O + N_2$	$1.8 \times 10^{-11} \exp(107/T)$	DeMore *et al.*, 1985	
R106)	$O(^1D) + O_2 \rightarrow O + O_2$	$3.2 \times 10^{-11} \exp(67/T)$	DeMore *et al.*, 1985	
R107)	$O + O_3 \rightarrow O_2 + O_2$	$8 \times 10^{-12} \exp(-2060/T)$	DeMore *et al.*, 1985	
R108)	$O + O + M \rightarrow O_2 + M$	2.76×10^{-34} $\exp(710/T)[M]$	Campbell and Thrush, 1967	
R109)	$O + O_2 + M \rightarrow O_3 + M$	$k_0 = 6 \times 10^{-34}$; $n = 2.3$ $k_\iota = 1 \times 10^{-10}$; $m = 0$	DeMore *et al.*, 1985	g
R110)	$CO + OH \rightarrow CO_2 + H$	1.5×10^{-13} $(1 + 0.6\ P_{atm})$	DeMore *et al.*, 1985	
R111)	$CO + O + M \rightarrow CO_2 + M$	6.5×10^{-33} $\exp(-2180/T)[M]$	Hampson and Garvin, 1977	
R112)	$H + CO + M \rightarrow HCO + M$	2×10^{-33} $\exp(-850/T[M]$	Baulch *et al.*, 1976	
R113)	$H + HCO \rightarrow H_2 + CO$	1.2×10^{-10}	Hochanadel *et al.*, 1980	
R114)	$HCO + HCO \rightarrow H_2CO + CO$	2.3×10^{-11}	Hochanadel *et al.*, 1980	
R115)	$OH + HCO \rightarrow H_2O + CO$	5×10^{-11}	Baulch *et al.*, 1976	
R116)	$O + HCO \rightarrow H_2O + CO$	1×10^{-10}	Hampson and Garvin, 1977	
R117)	$O + HCO \rightarrow OH + CO$	1×10^{-10}	Hampson and Garvin, 1977	
R118)	$O_2 + HCO \rightarrow HO_2 + CO$	$5.5 \times 10^{-11}\ T^{-0.4}$	Veyret and Lesclaux, 1980	
R119)	$H_2CO + H \rightarrow H_2 + HCO$	2.8×10^{-11} $\exp(-1540/T)$	DeMore *et al.*, 1985	
R120)	$H_2CO + OH \rightarrow H_2O + HCO$	1×10^{-11}	DeMore *et al.*, 1985	
R121)	$H_2CO + O \rightarrow HCO + OH$	$3 \times 10^{-11} \exp(-1550/T)$	DeMore *et al.*, 1985	
NO_x chemistry				
R122)	$NO + h\nu \rightarrow N + O$	$1.80 \times 10^{-6}\ s^{-1}$	Cieslik and Nicolet, 1973	k
R123)	$NO_2 + h\nu \rightarrow NO + O$	$6.34 \times 10^{-3}\ s^{-1}$	DeMore *et al.*, 1985	a
R124)	$HNO + h\nu \rightarrow H + NO$	$(= J_{HNO_2})$	See R125	d

Table II. (Continued).

	Reaction	Rate constant ($cm^3\ s^{-1}$)	Reference	Notes
R125)	$HNO_2 + h\nu \rightarrow OH + NO$	$1.7 \times 10^{-3}\ s^{-1}$	Cox, 1974	
R126)	$HNO_3 + h\nu \rightarrow OH + NO_2$	$1.15 \times 10^{-4}\ s^{-1}$	DeMore *et al.*, 1985	a
R127)	$N + O_2 \rightarrow NO + O$	$4.2 \times 10^{-12} \exp(-3220/T)$	DeMore *et al.*, 1985	
R128)	$N + OH \rightarrow NO + H$	5.3×10^{-11}	Baulch *et al.*, 1973	
R129)	$N + NO \rightarrow N_2 + O$	3.4×10^{-11}	DeMore *et al.*, 1985	
R130)	$NO + O_3 \rightarrow NO_2 + O_2$	$1.8 \times 10^{-12} \exp(-1370/T)$	DeMore *et al.*, 1985	
R131)	$NO + O + M \rightarrow NO_2 + M$	$k_0 = 9 \times 10^{-32}$; $n = 1.5$ $k_\infty = 3 \times 10^{-11}$; $m = 0$	DeMore *et al.*, 1985	g
R132)	$NO + HO_2 \rightarrow NO_2 + OH$	$3.7 \times 10^{-12} \exp(240/T)$	DeMore *et al.*, 1985	
R133)	$NO + OH + M \rightarrow HNO_2 + M$	$k_0 = 7 \times 10^{-31}$; $n = 2.6$ $k_\infty = 1.5 \times 10^{-11}$; $m = 0.5$	DeMore *et al.*, 1985	g
R134)	$NO_2 + O \rightarrow NO + O_2$	9.3×10^{-12}	DeMore *et al.*, 1985	
R135)	$NO_2 + H \rightarrow NO + OH$	$4.8 \times 10^{-10} \exp(-400/T)$	Clyne and Monkhouse, 1977	
R136)	$NO_2 + OH + M \rightarrow HNO_3 + M$	$k_0 = 2.6 \times 10^{-30}$; $n = 3.2$ $k_\infty = 2.4 \times 10^{-11}$; $m = 1.3$	DeMore *et al.*, 1985	g
R137)	$HNO_2 + OH \rightarrow H_2O + NO_2$	6.6×10^{-12}	Hampson and Garvin, 1977	
R138)	$HNO_3 + OH \rightarrow H_2O + NO_2 + O$	$k_0 = 7.2 \times 10^{-15} \exp(785/T)$ $k_2 = 4.1 \times 10^{-16} \exp(1440)$ $k_3 = 1.9 \times 10^{-33} \exp(725/T)$	DeMore *et al.*, 1985	l
R139)	$H + NO + M \rightarrow HNO + M$	$2.1 \times 10^{-32} \exp(300/T[M]$	Hampson and Garvin, 1977	
R140)	$HCO + NO \rightarrow HNO + CO$	$1.2 \times 10^{-10}\ T^{-0.4}$	Veyret and Lesclaux, 1980	
R141)	$H + HNO \rightarrow H_2 + NO$	$5 \times 10^{-13}\ T^{0.5} \exp(-1200/T)$	Baulch *et al.*, 1973	
R142)	$O + HNO \rightarrow OH + NO$	$(= k_{141})$		d
R143)	$OH + HNO \rightarrow H_2O + NO$	6×10^{-11}	Baulch *et al.*, 1973	

Notes to Table I

a Calculated from solar fluxes (WMO, 1985) and cross sections; diurnally-averaged values at 63.5 km in the standard model

b Presumed slow relative to reaction R38

c Assumed equal to J_{HCl}

d Estimated

e Theoretical estimate

f Excited S_2 states ignored

g Rate constant given by

$$k(M, T) = \left[\frac{k_0(T)\,[M]}{1 + k_0(T)[M]/k_\infty(T)}\right] 0.6^{\{1 + [\log_{10}(k_0(T)[M]/k_\infty(T)]^2\}^{-1}}.$$

h Assumed equal to rate for reaction of SO with ClO

i Assumed equal to rate for reaction of Br with H_2CO

j No recommendation given; value based on measurement by Langford and Oldershaw (1972)

k Band strengths modified to agree with Allen and Frederick (1982) at zero optical depth

l Products uncertain; rate constant given by

$$k(M, T) = k_0 + \frac{k_3[M]}{1 + k_3\,[M]/k_2}.$$

m Phillips *et al.* (1981) report absolute absorption cross sections for SO. I assumed that SO dissociates with unit efficiency, following Yung and DeMore (1982) and others. The actual quantum yield for dissociation is not known, but it is probably less than 0.1.

and various amounts of CO_2. 43 chemicals species were included: these are shown in Table I. They are divided into three groups: (1) long-lived species, for which both chemistry and transport were considered, (2) short-lived species, for which transport was neglected, and (3) inert, or relatively inert species, for which constant mixing ratios were assumed. The long-lived species group also includes short-lived species for which the chemistry is nonlinear. Reactions and rate constants linking these species are given in Table II.

The sulfur chemistry in the model is not as well understood as that of the C-H-O-N species. Since this study was performed, it has come to my attention that reaction (R4), photolysis of SO, may be substantially slower than assumed here. Other, hopefully less serious, problems with sulfur rate constants may exist. Such changes may affect the plausibility of a sulfur UV screen (Kasting *et al.*, 1989); however, they should not alter the general conclusions reached here, because no UV screen is assumed in this model. Sulfur chemistry does affect the atmospheric hydrogen budget, so some modification of the model's detailed photochemical predictions may be expected as our knowlege of sulfur photochemistry improves.

The vertical grid used in the model covers the region between 0 and 64 km in 1-km steps. Centered, second-order finite differences were used to transform the system of partial differential equations describing the chemistry and transport of the long-lived gases and particles into a set of coupled ordinary differential equations (ODE's). The ODE's were then integrated to steady state using the reverse Euler method (Dahlquist and Bjorck, 1974). The integrations were carried out for extremely long times (>10 million years) to obtain accurate convergence. Long integrations are required because the flux of CO into or out of the atmosphere is relatively small, whereas the atmospheric reservoir of CO is in some instances very large. Only in extreme cases, e.g. 10-bar, high-CO atmospheres, is the CO residence time so long that atmospheric composition may have failed to remain in dynamic equilibrium with the impact flux.

Lightning production of NO, O_2, and CO was included in the model. These species were assumed to be produced from N_2 and CO_2 by the overall reactions

$$2\,CO_2 \rightarrow 2\,CO + O_2$$
$$N_2 + 2\,CO_2 \rightarrow 2\,NO + 2\,CO\,.$$

Stoichiometry requires that the lightning production rates $\Phi_{lt}(i)$ of these species be balanced, i.e.

$$\Phi_{lt}(CO) = \Phi_{lt}(NO) + 2\,\Phi_{lt}(O_2)\,. \tag{6}$$

The production rate of NO was calculated by scaling from the modern atmosphere (Kasting, 1979), assuming a freeze-out temperature of 3500 K and a present-day, column-integrated NO source of 10^9 molecules $cm^{-2}\ s^{-1}$ (Borucki and Chameides, 1984). The O_2 production rate was scaled to NO production using the relative equilibrium abundances of O_2 and NO at 3500 K. Lightning production of CO was calculated from Equation (6).

Rainout of soluble gases was parameterized using the method of Giorgi and Chameides (1985). Significant uncertainties are involved in extrapolating to past atmospheres, especially ones that are warmer and denser than today's. Under these conditions, the tropopause moves upward to higher altitudes, so it is clearly unrealistic to assume the same altitude dependence for the rainout rate that is used at 1 bar. This problem was revolved by 'stretching' the rainout profile to match the calculated height of the troposphere, that is, by assuming that the rainout rates at the bottom and top of the troposphere are the same as at present (~5 and 100 days, respectively, for highly soluble species and longer for weakly soluble ones).

Photolysis rates were calculated using the Rayleigh scattering method of Yung (1976). A fixed solar zenith angle of 50° was assumed, and photolysis rates were multiplied by 0.5 to account for diurnal averaging.

b. Boundary conditions

Much of what happens in the model is determined by the boundary conditions imposed at the surface. There, soluble gases with no surface sources were assigned deposition velocities between 0 and 1 cm s^{-1}, following the approach of Slinn *et al.* (1978) and Lee and Schwartz (1981). SO_2 was assumed to have a fixed upward flux of 3.5×10^9 cm^{-2} s^{-1}, or about three to four times the modern volcanic sulfur release rate (Berresheim and Jaeschke, 1983).

Two types of lower boundary conditions were used for CO. In some simulations, the surface CO flux was set equal to the estimated present volcanic CO flux of 1×10^9 cm^{-2} s^{-1} (Holland, 1978). In most cases, however, the surface mixing ratio was specified, and the corresponding outgassing flux was calculated by the model. This procedure speeded model convergence and allowed the identification of multiple-valued solutions, in which a given CO production rate supports several different atmospheric CO mixing ratios.

H_2 was accorded a convoluted, but nonetheless self-consistent, treatment. To avoid including molecular diffusion, hydrogen escape was simulated by allowing H_2 to flow into the ground with a deposition velocity $v_{dep}(H_2) = 2.5 \times 10^{13}/n_0$ cm s^{-1}, where n_0 is the total surface number density in molecules cm^{-3}. (Allowing hydrogen to flow out the top of the grid without including molecular diffusion produces an unrealistic gradient in the H_2 profile). The downward flux of hydrogen is then $v_{dep}(H_2)n(H_2) = 2.5 \times 10^{13} f(H_2)$, which is equal to the diffusion-limited escape flux (see below) provided that H_2 is the dominant hydrogen-containing species in the stratosphere. Volcanic outgassing of H_2 was simulated by distributing an H_2 source throughout the lowest 10 km of the atmosphere. Since H_2 is well-mixed in all of these simulations, it makes little difference where the hydrogen is injected or whether it escapes from the top or the bottom of the atmosphere.

In most of the simulations, the assumed H_2 outgassing rate was 2.5×10^{10} cm^{-2} s^{-1}. This produces an atmospheric H_2 mixing ratio of $\sim 10^3$, near the upper end of the range (10^{-5} to 10^{-3}) used in previous studies (e.g. Yung and McElroy, 1979; Pinto *et al.*, 1980; Levine and Augustsson, 1985; Kasting *et al.*, 1984, 1990). This

outgassing rate is near the upper limit of the flux that might reasonably have been produced by early volcanos (Walker, 1977) and by photostimulated reduction of ferrous iron in the surface ocean (Braterman *et al.*, 1983).

c. Variable parameters

We do not know how much carbon the early atmosphere contained. A reasonable lower limit on pCO_2 is 0.2 bar, the amount necessary to compensate for the reduced luminosity of the young sun (Kasting *et al.*, 1984). A reasonable upper limit is 10 bar, the amount in the Walker (1985) global ocean model. To span this range, photochemical calculations were performed for combined (CO_2 + CO) partial pressures of 0.2, 2, and 10 bar. The N_2 partial pressure was held constant at 0.8 bar, so the total surface pressure in these models (including H_2O) was 1.0, 2.9, and 11.4 bar, respectively. Temperature profiles for the three models were calculated using the one-dimensional climate model of Kasting and Ackerman (1986). The solar constant was assumed to be equal to 75% of its present value, a figure which should have obtained around 4.0 Ga before present (Gough, 1981).

Calculated surface temperatures for the 0.2 bar, 2-bar, and 10-bar cases were 278 K, 317 K, and 360 K, respectively. Vertical temperature profiles are shown in Figure 1a. These profiles are idealizations of the actual temperature profiles calculated by the climate model. In particular, the stratospheric temperature was fixed at 180 K in all three cases. The predicted stratospheric temperatures ranged from 160 K to 220 K; however, these values are not reliable because Doppler broadening is handled rather crudely in the Kasting and Ackerman climate model.

Eddy diffusion profiles used in the three models are shown in Figure 1b. The profile for the 0.2-bar (CO_2 + CO) model was taken from Massie and Hunten (1981) and is appropriate for the modern atmosphere. For the 2- and 10-bar models, the profile was shifted upward by 4 km and 11 km, respectively, and an eddy diffusion coefficient (K_{edd}) of 10^5 cm^2 s^{-1} was assigned to the lowermost grid points. The shifted profiles are consistent with the change in tropopause altitude predicted by the climate model; they preserve roughly the same variation of K_{edd} with pressure as is observed in the modern stratosphere. Whether K_{edd} would have been significantly different in the absence of a stratospheric temperature inversion, and how it might actually vary with surface pressure, is unknown. Some sensitivity calculations were performed using higher K_{edd} values in the lower stratosphere to determine what effect this would have on the results.

A third factor that was varied was the water vapor distribution. In the 0.2- and 2-bar (CO_2 + CO) simulations, the tropospheric relative humidity was assumed to be given by the formula of Manabe and Wetherald (1967)

$$r = \frac{0.77\ (P/P_s - 0.02)}{(1 - 0.02)} \tag{7}$$

where P represents pressure and P_s is the pressure at the surface. For the 10-bar

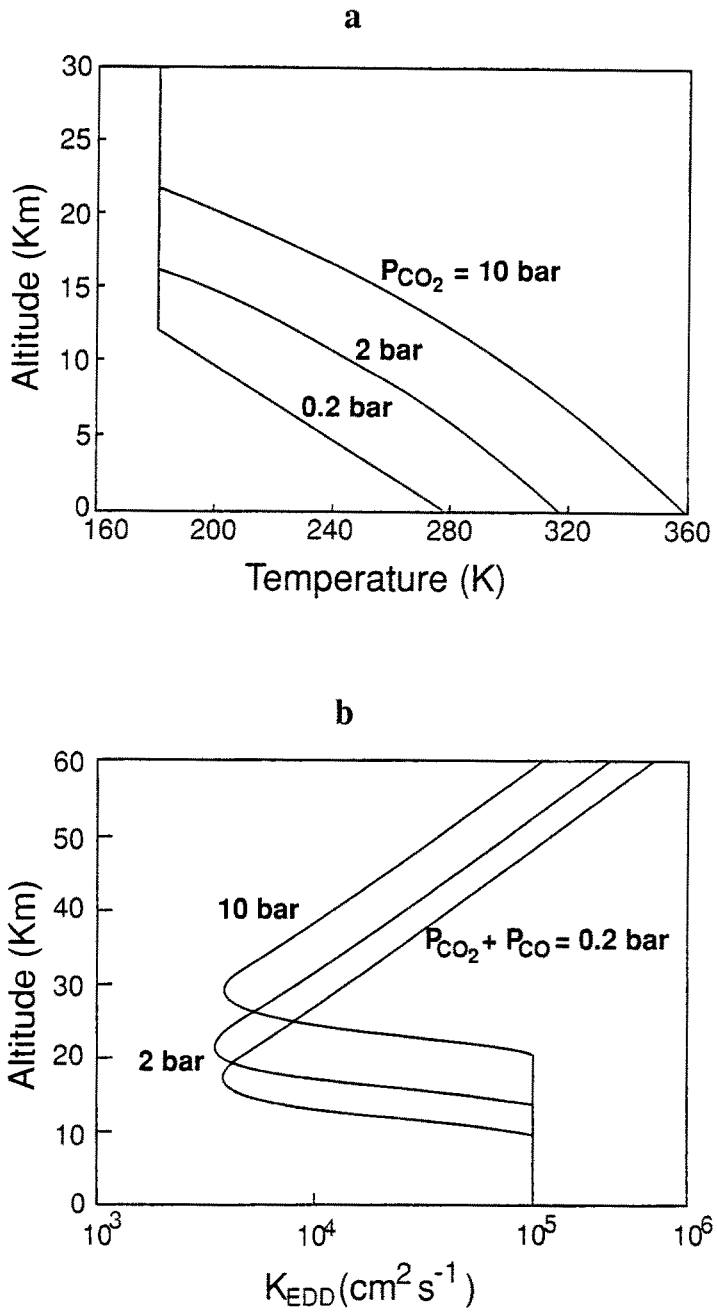

Fig. 1. Temperature (a) and eddy diffusion (b) profiles used in the photochemical model calculations. Temperatures were calculated using the climate model of Kasting and Ackerman (1986), assuming 75% of present solar luminosity. The N_2 partial pressure is 0.8 bar in all three cases. The eddy diffusion profile used for the 0.2-bar (CO_2 + CO) case is similar to that in the modern atmosphere.

simulation, the same formula was used, but a minimum relative humidity of 0.15 was specified to prevent the upper troposphere from becoming unrealistically dry.

Finally, different rates of NO production were assumed in the models (Figure 2). Column NO production in the 0.2-bar (CO_2 + CO) simulations was about half the present value, or 5×10^8 cm^{-2} s^{-1}, at low CO/CO_2 ratios. This is the amount expected from lightning alone. This rate decreases at high CO/CO_2 ratios as the availability of oxygen atoms declines. Column NO production for the 2-bar (CO_2 + CO) atmosphere was a factor of four higher; this is roughly the amount predicted for impacts at 4.0 Ga using Prinn and Fegley's efficiency factor. The 10-bar (CO_2 + CO) simulations were performed for two different NO production rates: 6×10^8 cm^{-2} s^{-1} ('low-NO') and 6×10^9 cm^{-2} s^{-1} ('high-NO'). The first case corresponds to zero impact production of NO, the second to a fairly substantial impact production rate. As shown below, NO production has a pronounced effect on atmospheric chemistry, particularly at high (CO_2 + CO) levels.

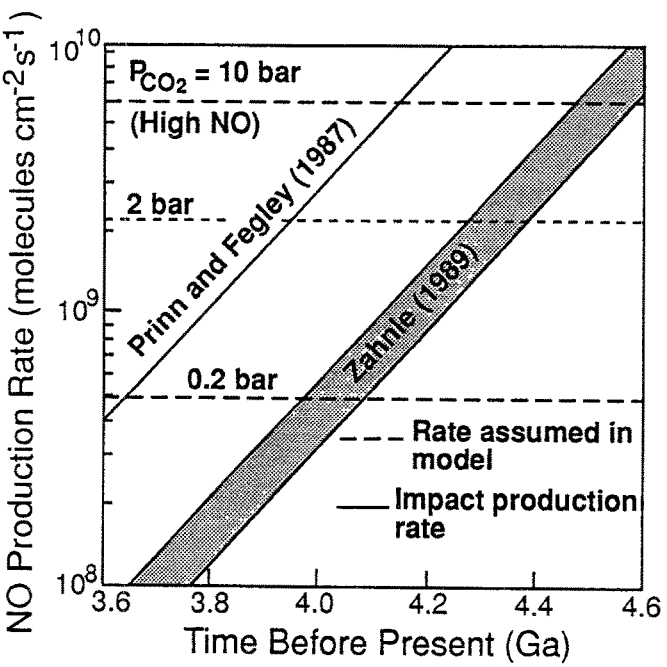

Fig. 2. NO shock production rates assumed in the models (dashed lines) versus NO impact production rates estimated in Section 2c (solid lines). Values shown are appropriate for low CO/CO_2 ratios; NO production decreases at higher CO concentrations. The shaded area represents the range of NO production rates in the Zahnle (1989) model for different assumptions concerning the size of the largest impactor (see text).

4. Photochemical Results

a. Base-case model

A 'base-case' simulation, so labelled because it is similar in many respects to previous models (e.g. Kasting *et al.*, 1984) is shown in Figure 3. The assumed CO_2 partial pressure is 0.2 bar. CO and H_2 were assigned outgassing rates of 1×10^9 cm^{-2} s^{-1} and 2.5×10^{10} cm^{-2} s^{-1}, respectively. Major atmospheric constituents are shown in Figure 3a. N_2 and CO_2 are dominant, as in earlier models. O_2 is relatively abundant up high, where it is produced from CO_2 dissociation, but disappears at low altitude because of reactions with H and HCO (R89 and R118). The calculated CO/CO_2 ratio is 4×10^{-4}.

Figures 3b-d show the other important species in the model. H_2S is more abundant than SO_2 near the surface (Figure 3b), even though it has no assumed surface source, because it is photochemically longer-lived in the reducing lower atmosphere. Formaldehyde (H_2CO) is another relatively abundant reduced species (Figure 3c). NO and HNO are the dominant odd nitrogen compounds (Figure 3d) for reasons

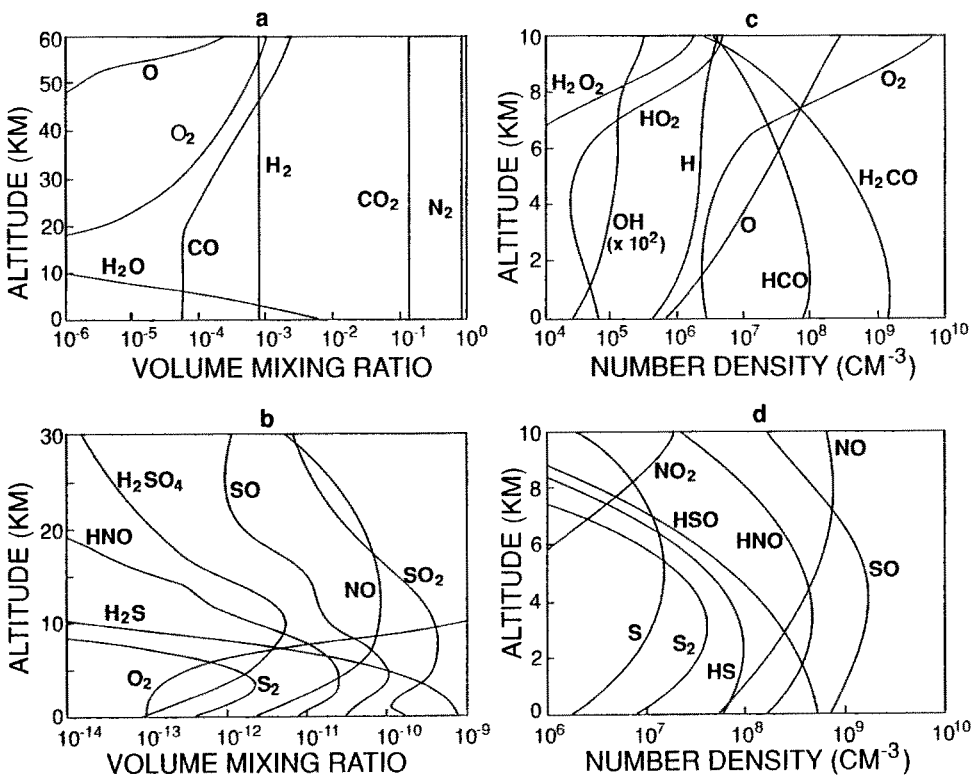

Fig. 3. Vertical profiles of selected species in the 'base-case' model. The total (CO_2 + CO) partial pressure is 0.2 bar, and the CO/CO_2 ratio is 5×10^{-4}; (a) major atmospheric constituents (b) long-lived sulfur and nitrogen species (+ O_2) (c) O_x, HO_x and H_xCO species (d) sulfur and nitrogen number densities.

discussed by Kasting and Walker (1981). HCO and HS are the most important reducing radicals.

b. Calculations at different (CO_2 + CO) levels

The main computational part of this study consists of a series of model calculations at combined (CO_2 + CO) pressures of 0.2, 2, and 10 bar. The lower boundary condition on CO for these simulations was constant mixing ratio. Solutions were obtained for a wide range of CO/CO_2 ratios by performing calculations for different CO mixing ratios. When utilized in this manner, the photochemical model calculates the CO source, $\Phi_{out}(CO)$, required to sustain a given atmospheric CO/CO_2 ratio. Although this source appears as a surface flux in the model, it includes both volcanic outgassing and impact production. $\Phi_{out}(CO)$ is of necessity equal to the net photochemical destruction rate of CO, i.e. column loss less column production.

In performing these calculations, it is instructive to keep track of the atmospheric hydrogen budget, that is, the net inflow and outflow of H_2. The hydrogen budget is defined by the equation

$$\Phi_{out}(H_2) + \Phi_{out}(CO) = \Phi_{esc}(H_2) + \Phi_{in}(H_2) \,. \tag{8}$$

The terms on the left represent sources of reduced gases; the terms on the right are hydrogen loss processes. $\Phi_{esc}(H_2)$ is the diffusion-limited hydrogen escape rate, given by

$$\Phi_{esc}(H_2) \approx 2.5 \times 10^{13} f_t(H_2) \text{ molecules cm}^{-2} \text{ s}^{-1} \,, \tag{9}$$

where $f_t(H_2)$ ($= f(H_2) + f(H_2O) + \frac{1}{2} f(H) + \ldots$) is the total hydrogen mixing ratio in the stratosphere (Hunten 1973; Walker, 1977). $\Phi_{in}(H_2)$ represents the net loss of atmospheric H_2 from rainout and surface deposition of soluble gases

$$\begin{aligned}\Phi_{in}(H_2) = {} & 2\,\Phi_r(H_2CO) + 3\,\Phi_r(H_2S) + 3/2\,\Phi_r(HSO) + 5/2\,\Phi_r(HS) + \Phi_r(CO) + \\ & + 16\,\Phi_r(S_8) - \Phi_r(H_2O_2) - 1/2\,\Phi_r(HNO) - \Phi_r(\text{Sulfate}) \,.\end{aligned} \tag{10}$$

Here, $\Phi_r(i)$ represents the combined rainout plus surface deposition rate of species i. It is assumed that all such species go into the ocean and are lost. $\Phi_{in}(H_2)$ is computed by defining reference oxidation states for hydrogen (H_2O), carbon (CO_2), nitrogen (N_2), and sulfur (SO_2), and then determining the number of hydrogen molecules taken up or released during the formation of each species. Direct rainout of (weakly soluble) H_2 is ignored on the grounds that the ocean would be saturated with hydrogen; thus, any loss from rainout should be balanced by outgassing from the ocean surface. Rainout of CO presents special problems that are discussed in the next section. For the moment, let us assume that CO behaves like H_2, i.e. there is no net transfer between the atmosphere and the ocean. Oxidation of rocks during weathering on land surfaces is neglected on the grounds that the continents would have been small and the atmospheric O_2 concentration would have been low (Figure 3c).

The basic results of the simulations are presented in Figures 4 and 5. Figure

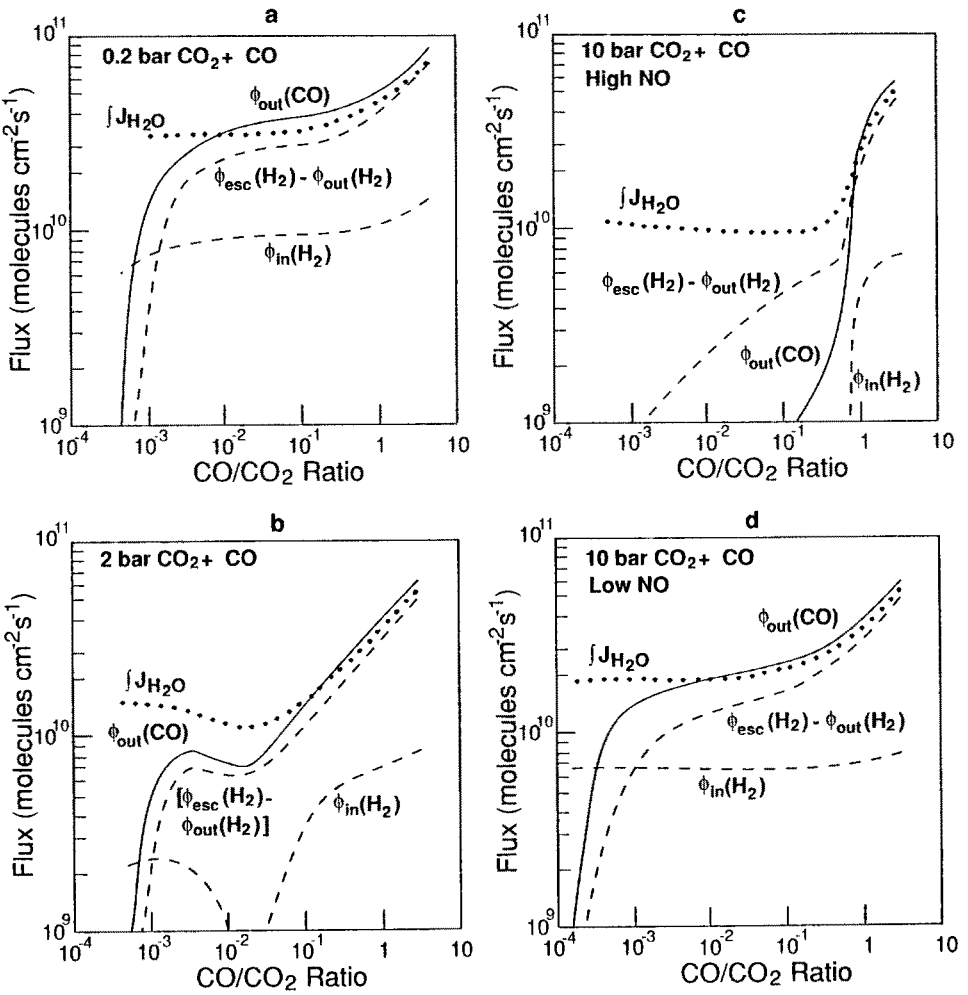

Fig. 4. Important factors in the hydrogen and CO budgets for the various model atmospheres. $\Phi_{out}(CO)$ is the CO flux required to sustain a given atmospheric CO/CO_2 ratio or, equivalently, the net photochemical destruction rate of CO. $\int J(H_2O)$ is the column-integrated H_2O photolysis rate: (a) 0.2-bar (CO_2 + CO) (b) 2-bar (CO_2 + CO) (c) 10-bar (CO_2 + CO), high NO (d) 10-bar (CO_2 + CO), low NO. High- and low-NO models are described in the text.

4 shows $\Phi_{out}(CO)$, along with other terms of importance in the hydrogen budget. The dashed curves represent the net H_2 rainout rate (Equation (10) and the difference between the escape rate and the assumed H_2 outgassing rate. Since Equation (8) must balance, the sum of the two dashed curves must be (and is in practice) equal to the solid curve. This, by the way, is a good test of one's photochemical model. Any imbalance in Equation (8) indicates either an inconsistency in the chemical reaction scheme or a violation of mass conservation.

Also shown in Figure 4 (dotted curves) is the column-integrated photolysis rate of water vapor [$\int J(H_2O)$]. In each case studied, $\Phi_{out}(CO) \approx \int J(H_2O)$ at high CO/

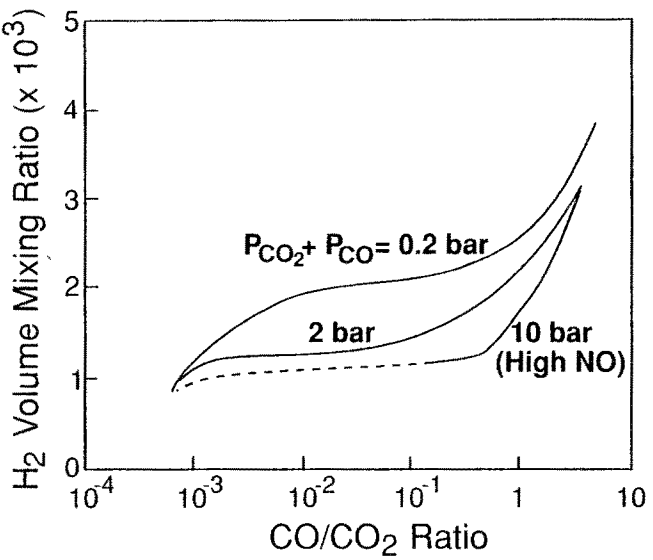

Fig. 5. Surface H_2 mixing ratios for the 0.2-bar, 2-bar, and 10-bar (high-NO) models. The dashed portion of the 10-bar model is physically inaccessible because the required CO flux is negative (Figure 5c). The H_2 outgassing rate is fixed at 2.5×10^{10} cm^{-2} s^{-1} in all of the calculations.

CO_2 ratios. This result is a direct consequence of the reaction of CO with OH (R110). At high atmospheric CO mixing ratios, virtually every OH radical produced by H_2O photolysis reacts with CO, releasing H atoms which ultimately recombine to form H_2. Nearly all of this H_2 escapes to space because there is little OH available to react with. At low CO mixing ratios, $\Phi_{out}(CO) \neq \int J(H_2O)$ because some OH radicals do react with H_2. The chemistry in this model is complicated by the fact that CO can also be oxidized by O atoms produced from SO_2 photolysis. This explains why $\Phi_{out}(CO)$ is, in general, slightly higher than $\int J(H_2O)$.

Figure 5 shows atmospheric H_2 mixing ratios corresponding to Figure 4a–c. H_2 mixing ratios increase with increasing CO/CO_2 ratio as a consequence of the (implicit) increase in $\Phi_{out}(CO)$. At low CO/CO_2 ratios, the H_2 mixing ratio is $\sim 10^{-3}$ – the value predicted by Equation (8) if rainout is neglected. The left-hand portion of the 10-bar (CO_2 + CO) curve is dashed to indicate that this region is physically inaccessible because $\Phi_{out}(CO)$ is negative, i.e. the rate of photochemical production of CO exceeds its loss.

c. Importance of NO

Perhaps the most interesting photochemical result of this study is the large effect of NO on the atmospheric oxidation state, particularly for dense CO_2 atmospheres. This effect is illustrated by the difference between Figure 5a, b, and d, on the one hand, and Figure 5c on the other. For the 0.2- and 2-bar (CO_2 + CO) simulations, and for the 'low-NO', 10-bar model, the atmosphere remains relatively undissociated

at low CO input rates. Predicted ground-level CO/CO_2 ratios for the present volcanic CO flux are 4×10^{-4}, 5×10^{-4}, and 1.6×10^{-4}, respectively. For the 'high-NO', 10-bar case (Figure 5c), the corresponding CO/CO_2 ratio is 0.14 – almost 1000 times higher. Thus, these calculations indicate that a dense primitive atmosphere could have had a high CO/CO_2 ratio if NO was relatively abundant. (A caveat must be added here: Hydration of CO in the oceans may have kept the CO abundance low. See discussion in next section.) Sensitivity studies confirm that it is the additional NO that makes the difference, rather than the O_2 or CO produced by the shocks. This prediction, unlike other results to follow, does not depend on increased rates of CO input from volcanos or impacts. The effect of NO is much weaker at lower CO_2 levels; increasing NO by a factor of 10 in the 'base-case' model (Section 4a) increases the CO/CO_2 ratio by only about 50%.

The importance of NO apparently stems from its interactions with soluble gases affected by rainout. In most cases studied, reduced gases and particles are removed more rapidly than are oxidized species. However, the addition of NO creates highly soluble HNO by way of the fast reaction

$$NO + HCO \rightarrow HNO + CO . \qquad \text{(R140)}$$

HNO is an oxidized species (relative to N_2), so removal of HNO generates hydrogen, thereby lessening the demand for H_2 and CO in Equation (8). Consequently, a given CO/CO_2 ratio can be maintained by a smaller influx of CO. Furthermore, by destroying HCO, NO decreases the rate at which SO is reduced to HSO

$$SO + HCO \rightarrow HSO + CO . \qquad \text{(R32)}$$

This, in turn, causes more of the outgassed SO_2 to be converted to sulfate and less to S_8 or H_2S. This has the same general effect on the hydrogen budget as does rainout of HNO.

A related, but somewhat more subtle, effect of NO is to increase the effective lifetime of atmospheric SO_2. It does this by changing the sulfur speciation and decreasing the overall rainout rate of soluble sulfur gases. The SO_2 concentration becomes large enough in the 'high-NO' model to begin to shield tropospheric water vapor from photolysis. (Compare $\int J H_2O$ in Figure 4c and d.) This, in turn, reduces the production rate of OH radicals, thereby enhancing the photochemical lifetime of CO. Complex interactions such as this and the one discussed in the previous paragraph may require that both nitrogen and sulfur photochemistry be included in future models of the primitive atmosphere.

d. Sensitivity studies

A number of additional model simulations were performed to determine whether the high CO/CO_2 ratio predicted for the 'high-NO', 10-bar (CO_2 + CO) atmosphere is sensitive to factors other than NO. Most of these tests were performed for a fixed CO/CO_2 ratio of 0.32. In the 'high-NO' model, this corresponds to a CO outgassing rate of 1.75×10^9 cm^{-2} s^{-1}, or roughly twice the modern value. This

is probably a lower limit on the volcanic CO flux early in Earth's history and, hence, a lower limit on the atmospheric CO/CO_2 ratio in this model.

The first test was to vary the outgassing rate of H_2 from its nominal value of 2.5×10^{10} cm^{-2} s^{-1}. All other factors being equal, reducing $\Phi_{out}(H_2)$ should increase $\Phi_{out}(CO)$, since they both appear on the left hand side of Equation (8). All other factors are not equal, however. Decreasing $\Phi_{out}(H_2)$ to zero decreases the atmospheric H_2 mixing ratio by a factor of about 6. (Rainout of oxidized gases prevents H_2 concentrations from dropping any further.) The net effect is to reduce the required CO flux by about 50%. Increasing $\Phi_{out}(H_2)$ by a factor of 3 from its nominal value increases the required CO flux by about 30%. Neither of these changes is significant. The required CO flux does not change sign, nor does it do so when the same test is performed at lower CO/CO_2 ratios. At high CO/CO_2 ratios, $\Phi_{out}(CO)$ depends primarily on the photolysis rate of H_2O (Figure 5), which is insensitive to the atmospheric H_2 level. I conclude that variations in the H_2 outgassing rate, or in production of H_2 from other sources (e.g. impacts), should not alter the prediction of high CO/CO_2 ratios under these circumstances.

A second test was to increase the eddy diffusion coefficient in the model stratosphere to a constant value of 10^5 cm^2 s^{-1} below 60 km. An increase of this nature is possible, given the absence of a temperature inversion in the stratosphere (Figure 1a). For a CO/CO_2 ratio of 0.32, the effect was to increase $\Phi_{out}(CO)$ by about 50%. At $CO/CO_2 = 5 \times 10^{-4}$, the effect was to decrease the downward CO flux by 15%. Once again, the changes are relatively insignificant. Modest variations in K_{EDD} apparently have little effect on the atmospheric CO/CO_2 ratio.

Many other factors in the model could be varied without violating any known constraints on the early atmosphere or on our present understanding of chemical kinetics. Any changes that significantly alter the atmospheric photochemistry could also alter the CO/CO_2 ratio. Thus, the prediction of a high CO/CO_2 ratio in the 10-bar, 'high-NO' model cannot be considered robust, despite the fact that it is insensitive to the changes considered here. The significant result is that a high CO/CO_2 ratio is possible, not that it is guaranteed.

5. Discussion

a. Atmospheric CO/CO_2 ratio versus time

By comparing the CO column loss rates, i.e. $\Phi_{out}(CO)$, from Figure 4 with the CO production rates calculated in Section 2, one can estimate the effect of impacts on the atmospheric CO/CO_2 ratio. Figure 6a shows this comparison for the 0.2-bar and 2-bar (CO_2 + CO) models. The CO production rates (dashed lines) are plotted as a function of time, while the CO loss rates (solid curves) are plotted as a function of atmospheric CO/CO_2 ratio. The graph is interpreted in the following manner: Suppose that one wants to determine the CO/CO_2 ratio at 4.2 Ga for the case of Cl chondrites impacting into a 0.2-bar (CO_2 + CO) atmosphere. Reading

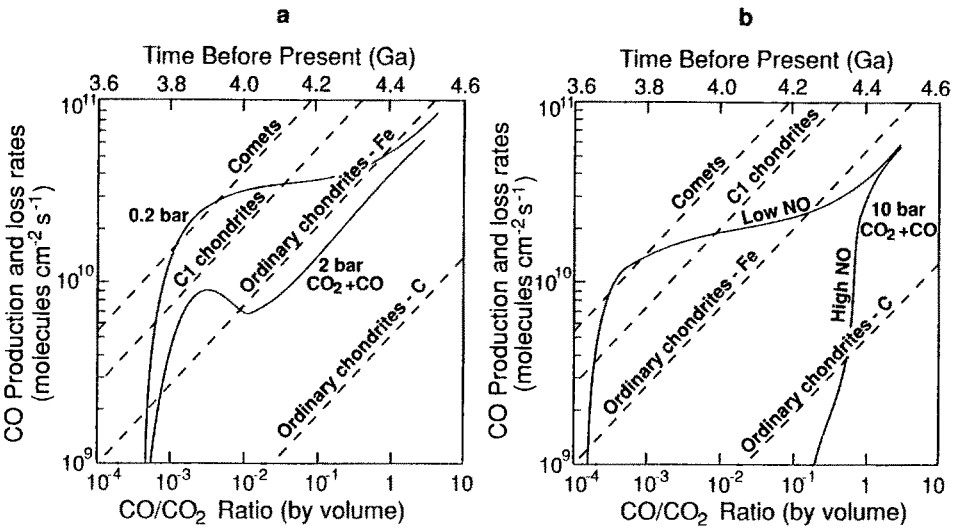

Fig. 6. CO production and loss rates for the various models. The loss rates (solid curves) are plotted as a function of atmospheric CO/CO_2 ratio. The production rates (dashed lines) are plotted against time. Comparing the two allows one to estimate the atmospheric CO/CO_2 ratio as a function of time (see text): (a) 0.2-bar and 2-bar (CO_2 + CO) models (b) 10-bar, high- and low-NO models.

down from the top at 4.2 Ga until one intersects the proper dashed line, one finds that the CO production rate is 5.5×10^{10} cm^{-2} s^{-1}. Moving horizontally to the right until one intersects the proper solid curve, and then reading down from there to the scale on the bottom of the figure, yields a corresponding atmospheric CO/CO_2 ratio of ~1.3. The actual CO/CO_2 ratio for this case might be even higher than this, since volcanic outgassing of CO is not included in this analysis.

Figure 6a indicates that, for these modestly dense atmospheres, impact of volatile-rich bodies (Cl chondrites or comets) could have significantly enhanced the CO/CO_2 ratio prior to ~3.8 Ga. CO/CO_2 ratios exceeding unity are possible at any time prior to 4.0 Ga in the most favorable case, that of comets impacting into a 2-bar (CO_2 + CO) atmosphere. Impact of volatile-poor, ordinary chondritic material would have been important only if a significant fraction of the metallic iron in these bodies reacted with ambient atmospheric CO_2.

Figure 6b shows the same comparison for the 10-bar (CO_2 + CO) model atmospheres. The two solid curves correspond to the 'high-NO' and 'low-NO' cases. In the 'high-NO' simulation, CO/CO_2 ratios approaching unity are possible at any time prior to 3.6 Ga, and possibly even later. Clearly, one needs to know the shock production rate of NO if one hopes to predict the CO/CO_2 ratio in such an atmosphere.

One general conclusion from this analysis is that no single model will suffice to describe the oxidation state of Earth's primitive atmosphere. Since the impact flux is time-dependent, and since it could have had a significant effect on atmospheric composition, the atmospheric CO/CO_2 ratio should have evolved with time in the

direction of increasing oxidation.

b. EFFECT OF CO REACTIONS IN THE OCEAN

As mentioned in Section 4b, the discussion to this point has assumed that dissolved CO does not react, so that there is no net transfer of CO between the atmosphere and oceans. In actuality, CO could have undergone a variety of aqueous phase chemical reactions that might invalidate this assumption. I have chosen to separate this topic from the remainder of the discussion because it is not clear how rapidly these aqueous reactions would have occurred or what the products would have been. Hence, any modeling of these processes must be at best semi-quantitative.

The initial reaction of dissolved CO is hydration to give formate ion (Van Trump and Miller, 1973; see also the Appendix to this paper)

$$CO(g) + OH^- \rightleftarrows HCOO^-(aq)$$

The kinetics of this reaction are known: the rate is inversely proportional to $[OH^-]$ and, thus, depends on ocean pH. It is also highly temperature dependent and would therefore have proceeded more rapidly if the early oceans were warm. One can demonstrate the possible importance of CO hydration by examining its rate under conditions corresponding to the 0.2-bar and 10-bar (CO_2 + CO) model atmospheres.

I assume here that the temperature of the ocean was the same as the global average surface temperatures shown in Figure 1a. Ocean pH must also be specified in order for the reaction rate to be computed. For the sake of specificity, I choose a pH of 7.2 in the 0.2-bar case and 4.2 in the 10-bar case. The ocean must have been somewhat more acidic than today under a moderately high-CO_2 atmosphere in the Archean to satisfy the constraints provided by evaporite deposits (Walker, 1983). An ocean-covered Earth with a 10-bar CO_2 atmosphere must have had very low ocean pH (probably <6) to avoid unreasonably high dissolved bicarbonate and carbonate concentrations (Walker, 1985). It should be borne in mind that there is nothing magic about the pH values I have assumed; they are chosen simply to illustrate a point.

Given oceanic pH, one can calculate an effective deposition velocity for CO (see Appendix). The flux of CO into the ocean is then

$$\Phi_{dep}(CO) = v_{dep}(CO) n_0(CO) , \tag{11}$$

where $n_0(CO)$ is the CO number density at the surface.

$\Phi_{dep}(CO)$ is compared to the surface CO flux $\Phi_{out}(CO)$ derived without considering formate production in Figure 7. In the cold, 0.2-bar (CO_2 + CO) simulation, $\Phi_{dep}(CO) \ll \Phi_{out}(CO)$ at all CO/CO_2 ratios. Thus, unless the oceanic pH was higher than assumed, hydration of CO should have been relatively unimportant, and the results shown in Figure 6a can be taken at face value. For the warm, 10-bar (high-NO) simulation, the results are just the opposite: $\Phi_{dep}(CO) \ll \Phi_{out}(CO)$ at all CO/CO_2 ratios. Unless the ocean pH was even lower than assumed, hydration of CO

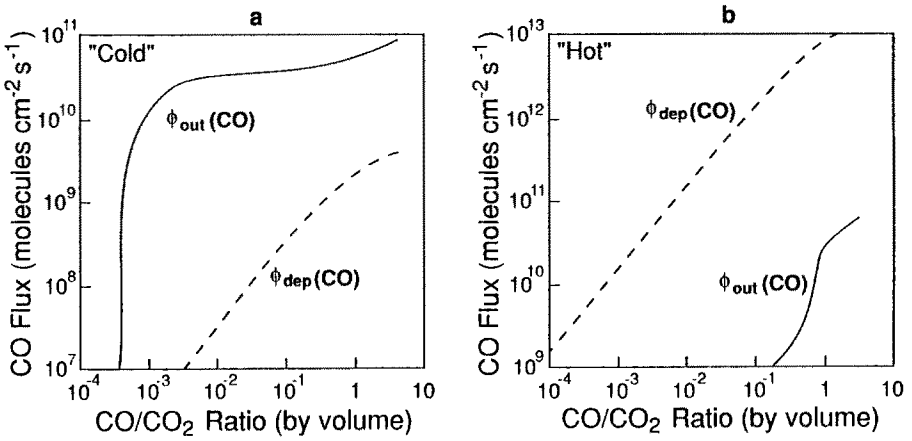

Fig. 7. CO loss rates caused by photochemistry [Φ_{out}(CO)] and by hydrolysis to formate [Φ_{dep}(CO)]. Whether or not hydrolysis is a net loss for CO depends on what happens to formate in the oceans: (a) 0.2-bar (CO_2 + CO) model (b) 10-bar, high-NO model.

would have been an important process.

In the latter case, or in any situation in which CO hydration is rapid, its effect on atmospheric composition depends on what happens to the formate ions created by the reaction of CO with OH^-. Formate in solution is thermodynamically unstable with respect to oxidation to bicarbonate

$$HCOO^- + H_2O \rightleftharpoons HCO_3^- + H_2 .$$

As far as I am aware, the kinetics of this reaction have not been studied, but it occurs within weeks to months in concentrated laboratory solutions (S. Miller, personal communication, 1989). Since H_2 can escape to the atmosphere and thence to space, this reaction should have a natural tendency to proceed to the right. In terms of the atmospheric CO budget, the formation of bicarbonate is equivalent to formation of CO_2; thus, oxidation of formate would increase the rate of CO production required to sustain a given CO/CO_2 ratio. If all of the formate in the 10-bar model decomposed in this manner, the atmospheric CO/CO_2 ratio would have been restricted to values below ~0.01, except possibly during the very earliest part of Earth's history. (Compare Figures 4d and 7b).

The primitive oceans need not have behaved like a laboratory bottle of formic acid, however. They probably contained significant quantities of ferrous iron, and they may have been irradiated from above by solar UV. Under these conditions, both formate and bicarbonate are reduced to formaldehyde and, possibly, to methane (Borowska and Mauzerall, 1988). The effect on the atmosphere depends on what products are formed and what happens to them next. Formaldehyde in solution hydrates to methylene glycol, $CH_2(OH)_2$ and then condenses to form sugars (Walker, 1964). Thus, impact-generated CO could conceivably have been converted directly into biological precursor molecules. This mechanism is potentially more efficient

than the atmospheric synthesis of formaldehyde (see next section). The atmospheric CO/CO_2 ratio would, in this case, have been low because CO would have been rapidly consumed.

If, on the other hand, most of the formate ends up as methane, the result would be quite different. Methane would have bubbled out of the oceans and been oxidized back to CO in the atmosphere (Kasting *et al.*, 1983; Zahnle, 1986). The system should then have behaved essentially as depicted in Figure 6: the atmospheric CO/CO_2 ratio could have been high, even if the rate of CO hydration was fast. Atmospheric photochemistry would have been somewhat more complicated, however, because of the presence of methane and its reaction products.

The general conclusion to be drawn here is that aqueous reactions of CO should have been important if the early Earth was warmer than today. They would have been marginally unimportant on a cold early Earth. Laboratory studies of UV-irradiated solutions containing ferrous iron, formate, and bicarbonate are needed to determine the fate of dissolved CO and CO_2.

c. Implications for the origin of life

Two fundamental precursor molecules for living systems are hydrogen cyanide (HCN) and formaldehyde (H_2CO). HCN (like NO) could have been produced by shock

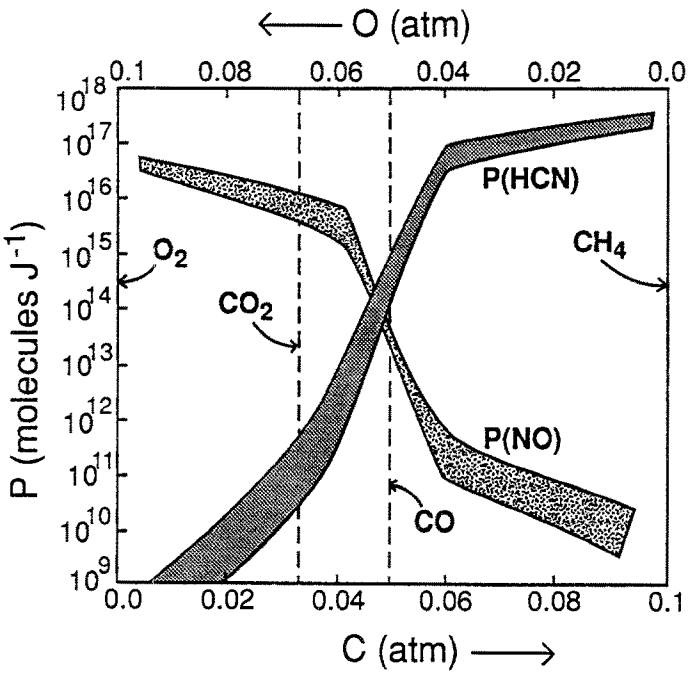

Fig. 8. Theoretically-predicted yields of HCN and NO for lightning-produced shocks in a one-bar atmosphere. The N_2 partial pressure is 0.9 bar; the rest of the atmosphere varies in composition from O_2 to CH_4 (after Chameides and Walker, 1981).

heating in lightning or impacts (Chameides and Walker, 1981; Fegley *et al.*, 1986; Stribling and Miller, 1987). If methane was present at the part per million level or higher, HCN could also have been produced by reactions of ionospherically-derived N atoms with the by-products of methane photolysis (Zahnle, 1986). Both of these mechanisms for HCN production would have operated more efficiently as the atmospheric CO/CO_2 ratio increased. Figure 8 shows theoretically-calculated HCN and NO production rates for shock-heating of an atmosphere containing 0.9 bar of N_2 and 0.1 bar of a second gas ranging in composition from O_2 to CH_4 (Chameides and Walker, 1981). In an N_2-O_2 atmosphere, the theoretically predicted yield is overwhelming NO; in an N_2-CH_4 atmosphere, HCN is produced. The C/O ratios of the model atmospheres considered here fall between the dashed vertical lines representing CO_2 and CO. Evidently, increasing the atmospheric CO/CO_2 ratio should increase the HCN yield; however, the theoretical yields are still relatively small for the atmospheres considered here.

Figure 8 is in qualitative agreement with preliminary experiments involving high energy spark discharges in different atmospheric mixtures (Stribling and Miller, 1989), although the experimental HCN yields in CO- or CO_2-dominated atmospheres are uncertain because they were near the detection limit for HCN. Lower energy experiments in which the shock heating was provided by a Tesla coil (simulating coronal discharge in the atmosphere) show a weaker dependence on the C/O ratio of the gas mixture. However, these experiments were performed at H/C ratios of unity or greater, which is much higher than the H/C ratios predicted for the early terrestrial atmosphere.

Zahnle's mechanism for HCN production is more promising. Methane would have been produced directly in the primitive atmosphere by photolysis of H_2O in the presenced of CO (Hubbard *et al.*, 1971; Bar-Nun and Hartman, 1978; Bar-Nun and Chang, 1983; Wen *et al.*, 1989). Wen *et al.* suggested a pathway for the reaction (through formaldehyde and methanol) and calculated atmospheric CH_4 mixing ratios for CO_2 partial pressures ranging from 3×10^{-4} to 1×10^{-2} atm. The highest CH_4 mixing ratio obtained was 4×10^{-8}, or roughly 100 times less than the amount needed for Zahnle's mechanism to become effective. The high-CO models studied here should have had greater methane production rates as a result of the greater abundance of CO and longer methane lifetimes because of the scarcity of OH. Methane may also have been produced in the oceans by reduction of bicarbonate and formate (Section 5b). This reaction could have taken place either in the surface ocean, under the stimulus of UV irradiation, or in the highly reducing ridge hydrothermal systems. If methane was produced at a significant rate in either the atmosphere or the ocean, Zahnle's mechanism could have generated substantial quantities of HCN.

Atmospheric synthesis of formaldehyde has been suggested as an early step in the origin of life (Pinto *et al.*, 1980). The rate at which formaldehyde was produced would have been a function of the atmospheric CO/CO_2 ratio. Formaldehyde removal rates (including rainout plus surface deposition) for the model atmospheres

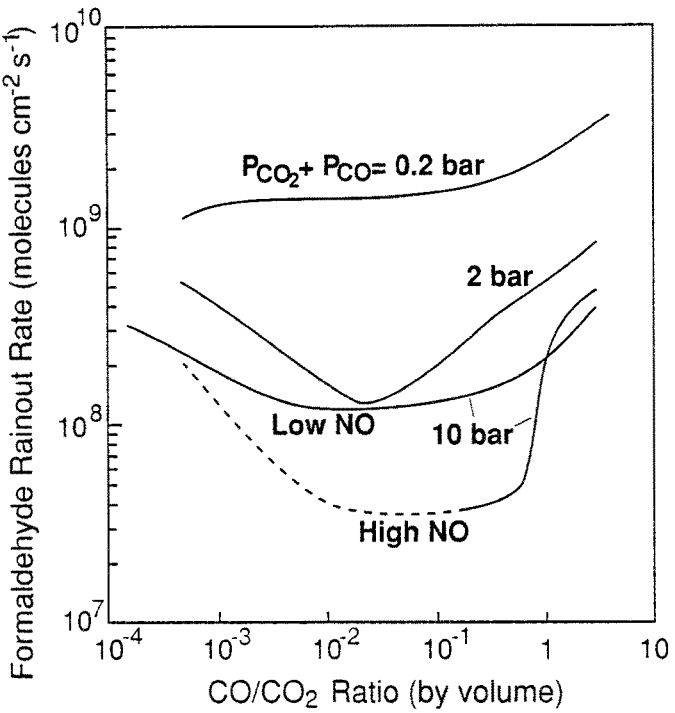

Fig. 9. Formaldehyde removal rates (rainout plus surface deposition) for the various model atmospheres. As in Fig. 5, the dashed portion of the 10-bar, high-NO curve is physically inaccessible.

studied are shown in Figure 9. The yield decreases as the atmosphere becomes denser because CO_2 photolysis takes place higher up; hence, less H_2CO is produced in the region where it can rain out. The H_2CO yield depends on the CO/CO_2 ratio in a complicated way. Modest increases in the CO/CO_2 ratio decrease the yield by destroying odd hydrogen (reactions R112 and R113); further increases enhance the yield by increasing the photolysis rate of H_2O. Figure 9 does not include formaldehyde produced by the photochemical reduction of bicarbonate and formate in the surface ocean. At high surface temperatures and high atmospheric CO/CO_2 ratios, reduction of dissolved formate would probably have been the dominant source of formaldehyde.

Taken together with the results of the last section, these considerations imply that the easiest time to originate life in surface environments may have been very early in the Earth's history. An atmosphere that was sufficiently reducing to facilitate prebiotic synthesis at, say, 4.3 Ga may have become too oxidizing by 3.8 Ga. The difference is caused by the decline in the impact flux. This prediction must, however, be weighed against the direct, detrimental effects of impacts on early life (Maher and Stevenson, 1988; Oberbeck and Fogleman, 1989; Sleep *et al.*, 1989). It may be that life could not have originated too early without being destroyed by impacts, but that it could not have originated too late because of a lack of impacts. If

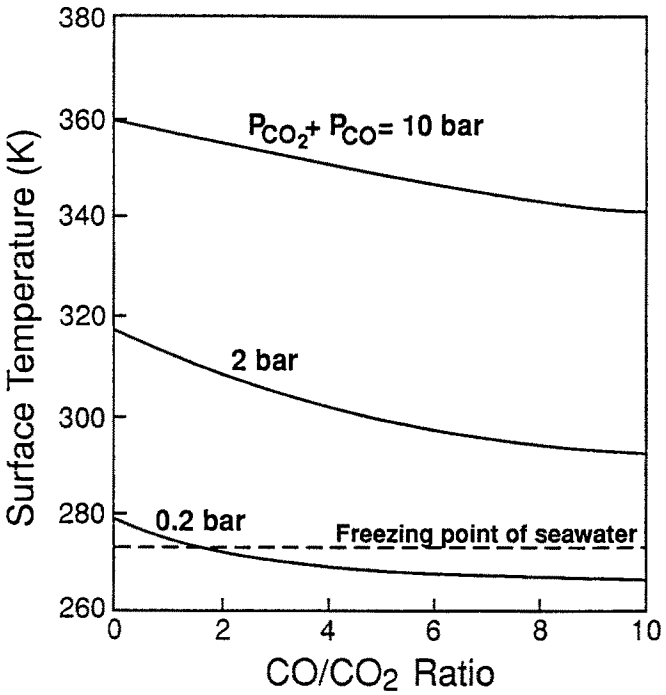

Fig. 10. Surface temperatures calculated for the various model atmospheres using the radiative-convective model of Kasting and Ackerman (1986). The solar flux is assumed to be 75% of its present value.

so, then the time window for the origin of life may have been narrow indeed.

Finally, impacts could also have altered the climate under which life originated. CO_2 is an excellent absorber of infrared radiation, whereas CO is not. Replacing CO_2 with CO would have decreased the atmospheric greenhouse effect, thereby lowering the surface temperature. The magnitude of the surface temperature decrease can be calculated with a one-dimensional climate model (Figure 10). This does not mean, however, that impacts would have cooled the early climate. Organic-rich impactors would have added carbon to the Earth's surface inventory, so their net effect during most of the heavy bombardment period would likely have been to heat the surface rather than to cool it. Cooling may have resulted prior to 4.3 Ga because of continuous stratospheric dust cover generated by very frequent impacts (Grinspoon and Sagan, 1987, 1990). Evidently climate, like atmospheric composition, should have undergone significant changes during the first half billion years of the Earth's history, but it is not easy to predict exactly what those changes would have been.

6. Conclusion

Photochemical modeling of possible primitive terrestrial atmospheres shows that impact production of CO and NO during the period prior to 3.8 Ga can have

a marked effect on atmospheric chemistry. The impact rate can be estimated from the lunar cratering record and from geochemical analysis of lunar rocks. The amount of CO produced depends on the types of bodies that were hitting the Earth; however, the production rate becomes large early in the Earth's history regardless of impactor composition. The amount of NO produced depends on the size distribution of the impactors; small bodies should produce NO more efficiently than large ones.

The CO/CO_2 ratio in the early atmosphere would have depended on a variety of factors, including the impact rate, impactor composition, atmospheric density, the atmospheric NO concentration, and the fate of dissolved formate in the ocean. Bombardment by comets or carbonaceous chondritic planetesimals could have produced CO/CO_2 ratios exceeding unity during the first half billion years of Earth's history if the climate was cool, so that formate production was slow, or if the decomposition of formate yielded reduced carbon compounds that were recycled to CO. Conversely, if formate decomposed primarily to bicarbonate, the CO/CO_2 ratio in a warm, dense atmosphere would have been low, regardless of the impact rate. Further progress in modeling the early atmosphere requires better knowledge of the chemical processing of atmospheric constituents in the primitive ocean.

Impacts may have facilitated the origin of life by increasing the production rates of hydrogen cyanide and formaldehyde. On the other hand, they may have hindered the evolution of life by their direct thermal effects. They would have affected climate by increasing the atmospheric CO/CO_2 ratio, by lofting dust into the stratosphere, and by augmenting the Earth's surface inventory of carbon. Including the effects of impacts in models of the early atmosphere permits a wide variety of conditions under which life might have originated.

Acknowledgments

I thank Kevin Zahnle, Stanley Miller, and David Mauzerall for helpful discussions of various aspects of this work. This work was supported by Grant # ATM–8901775 from the National Science Foundation and by Joint Research Interchange No. NCA2–369 with NASA Ames Research Center.

References

Allen, M. and Frederick, J. E.: 1982, *J. Atmos. Sci.* **39**, 2066.
Anders, E.: 1989, *Nature* **342**, 255.
Bar-Nun, A. and Chang, S.: 1983, *J. Geophys. Res.* **88**, 6662.
Bar-Nun, A. and Hartman, H.: 1978, *Origins of Life* **9**, 93.
Baulch, D. L. and Drysdale, D. D., and Horne, D. G.: 1976, *Evaluated Kinetic Data for High Temperature Reactions. Vol. 2*, Butterworths, London.
Baulch, D. L., Drysdale, D. D., Duxbury, J., and Grant, S.: 1976, *Evaluated Kinetic Data for High Temperature Reactions Vol. 3*, Butterworths, London.
Berresheim, H. and Jaeschke, W.: 1983, *J. Geophys. Res.* **88**, 3732.
Borowska, Z. and Mauzerall, D.: 1988, *Proc. Nat. Acad. Sci. U.S.A.* **85**, 6577.
Borucki, W. J. and Chameides, W. L.: 1984, *Rev. Geophys.* **22**, 363.
Braterman, P. S., Cairns-Smith, A. G. and Sloper, R. W.: 1983, *Nature* **303**, 163.
BVSP: 1981, Pergamon, New York.
Campbell, J. M. and Thrush, B. A.: 1967, *Proc. R. Soc. London, Ser. A.* **296**, 222.

Chameides, W. L. and Walker, J. C. G.: 1981, *Origins ofLife* **11**, 291.
Chang, S., DesMarais, D., Mack, R., Miller, S. L., Strathearn, G. E.: 1983, in J. W. Schopf (eds.), *Earth's Earliest Biosphere: Its Origin and Evolution*, Princeton University Press, Princeton, New Jersey, p. 53.
Chyba, C. F.: 1990, *Nature* **343**, 129.
Cieslik, S. and Nicolet, M.: 1973, *Planet. Space Sci.* **21**, 925.
Clyne, M. and Monkhouse, P.: 1977, *J. Chem. Soc. Farday Trans. II,* **73**, 298.
Cox, R. A.: 1974, paper presented at the LODATA Symposium on Chemistry of the Lower Atmosphere, Amer. Chem. Soc., Warrenton, VA.
Dahlquist, G. and Bjorck, A.: 1974, *Numerical Methods*, Prentice-Hall, Englewood Cliffs, New Jersey [trans. from Swedish by N. Anderson].
deAlmeida, A. A. and Singh, P. D.: 1986, *Earth, Moon, and Planets* **36**, 117.
DeMore, W. B., Margitan, J. J., Molina, M. J., Watson, R. T., Golden, D. M., Hampson, R. F., Kurylo, M. J., Howard, C. J., and Rvishankara, A. R.: 1985, *Chemical Kinetics and Photochemical Data for Use in Stratospheric Modeling*, Eval. No. 7, JPL Publication 85–37.
Fegley, B. Jr., Prinn, R. G., Hartman, H., and Watkins, G. H.: 1986, *Nature* **319**, 305.
Giorgi, F. and Chameides, W. L.: 1985, *J. Geophys. Res.* **90**, 7872.
Gough, D. O., 1981, *Solar Phys.* **74**, 21.
Grinspoon, D. H. and Sagan, C.: 1990, (in prep.)
Grinspoon, D. H. and Sagan, C.: 1987, *Bull. Am. Astron. Soc.* **19**, 872.
Hampson, R. F. and Garvin, D.: 1977, *Reaction Rate and Photochemical Data for Atmospheric Chemistry* , NBS Spec. Publ. U.S., 513.
Herron, J. T. and Huie, R. E.: 1980, *Chem. Phys. Lett.* **76**, 322.
Hills, H. A., Cicerone, R. J., Calvert, J. G., and Birks, J. W.: 1987, *J. Phys. Chem.* **91**, 1199.
Hochanadel, C. J., Sworski, T. J., and Ogren, P. J.: 1980, *J. Phys. Chem.* **84**, 231.
Holland, H. D.: 1984, *The Chemical Evolution of the Atmosphere and Oceans*, Princeton University Press, Princeton.
Holland, H. D.: 1978, *The Chemistry of the Atmosphere and Oceans*, Wiley, New York.
Holland, H. D.: 1962, in A. E. J Engel, H. L. James, B. F. Leonard (eds.) *Petrologic Studies: A Volume to Honor A. F. Buddington*, Geol. Soc. Am., New York, p. 447.
Hubbard, J. S., Hardy, J. P., and Horowitz, N. H.: 1971, *Proc. Nat. Acad. Sci.* **68**, 574.
Hunten, D. M.: 1973, *J. Atmos. Sci.* **30**, 1481.
Jessberger, E. K., Kissel, J. and Rahe, J.: 1989, in S. K. Atreya, J. B. Pollack, and M. S. Matthews (eds.), *Origin and Evolution of Planetary and Satellite Atmospheres*, University of Arizona Press, Tucson, p. 167.
Kasting, J. F.: 1979, '*Evolution of Oxygen and Ozone in the Earth's Atmospheree*', Ph.D. Dissertation, University of Michigan, Ann Arbor.
Kasting, J. F.: 1987, *Precambrian Res.* **34**, 205.
Kasting, J. F. and Ackerman, T. P.: 1986, *Science* **234**, 1383.
Kasting, J. F., Pollack, J. B., and Crisp, D.: 1984, *J. Atmos. Chem.* **1**, 403.
Kasting, J. F., Toon, O. B., and Pollack, J. B.: 1988, *Scientific Am.* **256**, 90.
Kasting, J. F. and Walker, J. C. G.: 1981, *J. Geophys. Res.* **86**, 1147.
Kasting, J. F., Zahnle, K. J., and Walker, J. C. G.: 1983, *Precambrian Res.* **20**, 121.
Kasting, J. F., Zahnle, K. J., Pinto, J. P., and Young, A. T.: 1990, *Origins of Life* **19**, 95.
Koster van Groos, A. F.: 1988, *J. Geophys. Res.* **93**, 8952.
Krankowsky, D. and Eberhardt, P.: 1988, in *Comet Halley 1986: World-Wide Investigations, Results and Interpretations*, Chicester: Ellis Horwood (in press).
Langford, R. B. and Oldershaw, G. A.: 1972, *J. Chem. Soc. Faraday Trans., I,* **68**, 1550.
Lee, Y. N. and Schwartz, S. E.: 1981, *J. Geophys. Res.* **86**, 11971.
Levine, J. S.: 1982, *J. Molec. Evol.* **18**, 161.
Levine, J. S. and Augustsson, T. R.: 1985, *Origins of Life* **15**, 299.
Lewis, J. S. and Prinn, R. G.: 1984, *Planets and Their Atmospheres: Origin and Evolution*, Academic Press, Orlando, Florida.
Maher, K. A. and Stevenson, D. J.: 1988, *Nature* **331**, 612.
Manabe, S. and Wetherald, R. T.: 1967, *J. Atmos. Sci.* **24**, 241.
Massie, S. T. and Hunten, D. M.: 1981, *J. Geophys. Res.* **86**, 9859.

McElroy, M. B., Kong, T. Y., and Yung, Y. L.: 1977, *J. Geophys. Res.* **82**, 4379.
McElroy, M. B., Wofsy, S. C., and Sze, N. D.: 1980, *Atmos. Environ.* **14**, 159.
McEwan, M. J. and Phillips, L. F.: 1975, *Chemistry of the Atmosphere*, Wiley, New York.
Melosh, H. J. and Vickery, A. M.: 1989, *Nature* **338**, 487.
Miller, S. L.: 1953, *Science* **117**, 528.
Miller, S. L.: 1955, *J. Am. Chem. Soc.* **77**, 2351.
Oberbeck, V. R. and Fogleman, G.: 1989, *Nature* **339**, 434.
Okabe, H.: 1971, *J. Amer. Chem. Soc.* **93**, 7095.
Oparin, A. I.: 1938, *The Origin of Life*, MacMillan, New York [Republished in 1953, New York, Dover].
Owen, T., Cess, R. D. and Ramanathan, V.: 1979, *Nature* **277**, 640.
Phillips, L.: 1981, *J. Phys. Chem.* **85**, 3994.
Pinto, J. P., Gladstone, C. R., and Yung, Y. L.: 1980, *Science* **210**, 183.
Prinn, R. G. and Fegley, B.: 1987, *Earth Planet. Sci. Lett.* **83**, 1.
Robinson, R. A. and Stokes, R. H.: 1959, *Electrolyte Solutions*, Butterworths, London, P. 363.
Rubey, W. W.: 1955, in A. Podervaart (eds.), *Crust on the Earth*, Geol. Soc. Am., New York, p. 631.
Rubey, W. W.: 1951, *Geol. Soc. Am. Bull.* **62**, 1111.
Safronov, V. S. and Ruzmaikina, T. v.: 1986, in D. Black, M. S. Matthews (eds.), *Protostars and Protoplanets II*, Univ. of Arizona Press, Tucson, p. 959.
Shemansky, D. E.: 1972, *J. Chem. Phys.* **56**, 1582.
Sleep, N. H., Zahnle, K. J., Kasting, J. F., and Morowitz, H. J.: 1989, *Nature* **342**, 139.
Slinn, W. G. N., Hasse, L., Hicks, B. B., Hogan, A. W., Lal, D., Liss, P. S., Munnich, K. O., Sehmel, G. A., and Vittori, O.: 1978, *Atmos. Environ.* **12**, 2055.
Stevenson, D. J.: 1983, in J. W. Schopf (eds.) *Earth's Earliest Biosphere: Its Origin and Evolution*, Princeton University Press, Princeton, New Jersey, p. 32.
Stribling, R. and Miller, S. L.: 1987, *Origins of Life* **17**, 261.
Stull, D. R. and Prophet, H.: 1971, *JANAF Thermochemical Tables*, NSRDS-NBS-37, U.S. Government Printing Office, Washington.
Sullivan, J. L. and Holland, A. C.: 1966, *NASA Tech. Rept.* CR371.
Thompson, B. A., Harteck, P. and Reeves, R. R., Jr.: *J. Geophys. Res.* **68**, 6431.
Toon, O. B., Kasting, J. F., Turco, R. P., and Liu, M. S.: 1987, *J. Geophys. Res.* **92**, 943.
Turco, R. P., Hamill, P., Toon, O. B., Whitten, R. C., and Kiang, C. S.: 1979, *J. Atmos. Sci.* **36**, 699.
Turco, R. P., Whitten, R. C., and Toon, O. B.: 1982, *Rev. Geophys.* **20**, 233.
Urey, H. C.: 1952, *The Planets: Their Origin and Development*, Yale University Press, New Haven, Conn.
Van Trump, J. E. and Miller, S. L.: 1973, *Earth Planet. Sci. Lett.* **20**, 145.
Veyret, B. and Lesclaux, R.: 1981, *J. Phys. Chem.* **85**, 1918.
von Zahn, U., Kumar, S., Niemann, H., Prinn, R.: 1983, in D. M. Hunten, L. Colin, T. M. Donahue, V. I. Moroz (eds.), *Venus*, University of Arizona Press, Tucson, p. 299.
Walker, J. C. G.: 1983, *Nature* **302**, 518.
Walker, J. C. G.: 1985, *Origins of Life* **16**, 117.
Walker, J. C. G.: 1977, *Evolution of the Atmosphere*, Macmillan, New York.
Walker, J. C. G., Hays, P. B., and Kasting, J. F.: 1981, *J. Geophys. Res.* **86**, 9776.
Walker, J. F.: 1964, *Formaldehyde*, Reinhold Publ. Co., New York.
Warneck, P., Marmo, F. F., and Sullivan, J. O.: 1964, *J. Chem. Phys.* **40**, 1132.
Wen, J.-S., Pinto, J. P., and Yung, Y. L.: 1989, *J. Geophys. Res.* **94**, 14957.
(submitted).
Wilhelms, D. E.: 1984, in M. H. Carr (ed.), *The Geology of the Terrestrial Planets*, NASA SP-469, p. 107.
WMO: 1985, World Meteorological Organization Rept. No. 16, *Atmospheric Ozone*, Vol. 1 (avail. from NASA, Earth Science and Applications Div.), Washington, D. C.
Yung, Y. L.: 1976, *J. Quant. Spectrosc. Radiat. Transf.* **16**, 755.
Yung, Y. L. and DeMore, W. B.: 1982, *Icarus* **51**, 199.
Yung, Y. L. and McElroy, M. B.: 1979, *Nature* **203**, 1002.
Zahnle, K. J.: 1990, *Global Catastrophes in Earth History*, ed. by V. Sharpton and P. Ward. Geol. Soc. o Amer. Special Paper, in press.
Zahnle, K. J.: 1986, *J. Geophys. Res.* **91**, 2819.

Appendix. Hydration of CO in the ocean

The largest single uncertainty in the model concerns the fate of CO dissolved in the primitive oceans. In the absence of competing processes, carbon monoxide in solution hydrates to give formic acid (Van Trump and Miller, 1973)

$$CO(g) + OH^- \rightleftarrows HCOO^-(aq) .$$

According to these authors, the lifetime of atmospheric CO against hydration can be written as

$$\tau_{CO}(yr) = 1/(k\alpha[OH^-] \times V_g/V_l \times 1/(8766 \text{ hr yr}^{-1}) \quad (A1)$$

where k is the rate constant for the hydration reaction in units of M^{-1} hr^{-1}, α is a dimensionless solubility coefficient for CO (equal to the normal Henry's Law constant multiplied by 22.4 moles l^{-1} atm^{-1}), $[OH^-]$ is the OH^- concentration in moles l^{-1}, V_g is the volume of the atmosphere in units of 1 cm^{-2}, and V_l (= 270 1 cm^{-2}) is the volume of the ocean. The coefficients k and α are given by

$$\log_{10} k = 15.83 - 4886/T \, M^{-1} \, hr^{-1} \quad (A2)$$

$$\log_{10} \alpha = -14.948 + 2142.3/T + 2.012 \times 10^{-2} \, T . \quad (A3)$$

The lifetime of CO against hydrolysis depends inversely on $[OH^-]$; thus, it can be calculated only if one knows the oceanic pH. Unfortunately, the pH of the early oceans is not well constrained. In order to generate actual numbers, I simply assume that the pH is 7.2 in the 0.2-bar (CO_2 + CO) model and 4.2 in the 10-bar model. To calculate $[OH^-]$, one must factor in the temperature dependence of the dissociation product for water (Robinson and Stokes, 1959)

$$pK_w = -6.0846 + 4471.33/T + 0.017053 \, T , \quad (A4)$$

which is accurate for temperatures up to about 250 °C.

TABLE III

Parameters for CO hydration calculations

	$pCO_2 + pCO$	
	0.2 bar	10 bar
T_s (K)	278	360
$pK(H_2O)$	14.74	12.47
Ocean pH	7.2	4.2
$[OH^-]$ (moles l^{-1})	3×10^{-8}	5×10^{-9}
V_g (1 cm^{-2})	842	8,650
α	2.25×10^{-2}	1.76×10^{-2}
k (M^{-1} hr^{-1})	1.80×10^{-2}	181
τ_{CO}(yr)	2.8×10^{7}	2.3×10^{5}
v_{dep}(CO) (cm s^{-1})	1×10^{-9}	8×10^{-8}

For modeling purposes, it is convenient to express the results of this calculation in terms of an effective deposition velocity for CO

$$v_{\mathrm{dep}}(\mathrm{CO}) = H_{\mathrm{a}}/\tau_{\mathrm{co}}(s)\,, \tag{A5}$$

where H_{a} is the atmospheric pressure scale height (in cm) and τ_{co} is expressed in seconds. Calculated deposition velocities and other parameters for the 0.2-bar and 10-bar models are given in Table 3. It should be emphasized that these numbers are merely representative, since they depend upon assumed values of oceanic pH.